

Efficient Differentially Private Fine-Tuning of LLMs via Reinforcement Learning

Afshin Khadangi, Amir Sartipi^{*}, Igor Tchappi^{*}, Ramin Bahmani, Gilbert Fridgen

SnT, University of Luxembourg

^{*}Equal Contribution

The tension between data privacy and model utility has become the defining bottleneck for the practical deployment of large language models (LLMs) trained on sensitive corpora including healthcare. *Differentially private* stochastic-gradient descent (DP-SGD) guarantees formal privacy, yet it does so at a pronounced cost: gradients are forcibly clipped and perturbed with noise, degrading sample efficiency and final accuracy. Numerous variants have been proposed to soften this trade-off, but they all share a handicap: their control knobs are hard-coded, global, and oblivious to the evolving optimisation landscape. Consequently, practitioners are forced either to over-spend privacy budget in pursuit of utility, or to accept mediocre models in order to stay within privacy constraints. We present **RLDP**, the first framework to cast DP optimisation itself as a closed-loop control problem amenable to modern deep reinforcement learning (RL). RLDP continuously senses rich statistics of the learning dynamics and *acts* by selecting fine-grained per-parameter gradient-clipping thresholds as well as the magnitude of injected Gaussian noise. A soft actor—critic (SAC) hyper-policy is trained *online* during language-model fine-tuning; it learns, from scratch, how to allocate the privacy budget where it matters and when it matters. Across more than 1 600 ablation experiments on GPT2-SMALL, LLAMA-1B, LLAMA-3B, and MISTRAL-7B, RLDP delivers **perplexity reductions of 1.3–30.5% (mean 5.4%) and an average 5.6% downstream utility gain**. RLDP reaches each baseline’s *final* utility after only 13%–43% of the gradient-update budget (**mean speed-up 71%**), all while honouring the same (ϵ, δ) -DP contract and exhibiting equal or *lower* susceptibility to membership-inference and canary-extraction attacks.

Date: July 31, 2025

Correspondence: Afshin Khadangi, afshin.khadanki@uni.lu

Code, Logs and Models: [GitHub](#), [W&B](#), [Hugging Face](#)

Homepage: <https://www.uni.lu/snt-en/>



1 Introduction

Modern large-scale language models (LMs) underpin a wide range of natural-language understanding and generation applications, from conversational agents and code assistants to clinical-note summarisation. The unprecedented predictive power of transformer architectures, however, is enabled by equally unprecedented volumes of training text, much of which is scraped, user-generated, or otherwise sensitive. This tension between leveraging data at scale and respecting the privacy of the individuals represented in that data has elevated *differential privacy* (DP) to a first-class requirement for the next generation of foundation models.

Differential-privacy-aware optimisation. The canonical recipe for private deep learning is **DP-SGD** (Abadi et al., 2016), which clips each example’s gradient to a global radius C before adding Gaussian noise of standard deviation σC . The privacy loss accrued across training is tracked by analytical accountants such as Rényi DP (Mironov, 2017), Gaussian DP (Dong et al., 2022), and the Poisson subsampled Rényi DP (Zhu and Wang, 2019). When applied to transformers, DP-SGD suffers from a stark *utility gap*: models trained under a reasonable budget (e.g. $\epsilon \leq 8$) can suffer significant downstream accuracy relative to non-private baselines (Li et al., 2021). The central culprit is the one-size-fits-all clip radius C : gradients in early attention blocks may saturate the bound while feed-forward layers receive negligible updates, or vice versa as training progresses.

Adaptive clipping heuristics. A fertile line of work seeks to reduce this inefficiency by adapting C to the empirical gradient distribution. ADACLIP (Pichapati et al., 2019) maintains an exponential-moving average (EMA) of per-coordinate gradients; (Andrew et al., 2021) extend this to per-layer norms, while AUTOCLIP (Bu et al., 2023) uses a single global clipping norm, estimated via the p -th quantile of update norms, applied uniformly across all parameters in each step. DC-SGD leverages differentially private histograms to estimate gradient norm distributions, dynamically adjusting the clipping threshold C to reduce hyperparameter tuning overhead Wei et al. (2025). It introduces DC-SGD-P and DC-SGD-E, which adjust C based on gradient norm percentiles or expected squared error minimization, achieving up to nine times faster hyperparameter tuning compared to standard DP-SGD. GEOCLIP introduces a geometry-aware framework for DP-SGD that clips and perturbs gradients in a transformed basis aligned with the gradient distribution’s geometry, adaptively estimating this transformation using noisy gradients without additional privacy cost (Gilani et al., 2025). It provides convergence guarantees and a closed-form solution for the optimal transformation, minimizing noise while controlling gradient clipping probability, thus improving the privacy-utility trade-off.

Complementing some of the previous approaches, PSAC (Xia et al., 2023) eliminates the need for manually tuned constant clipping thresholds. Instead, PSAC introduces a non-monotonic adaptive weight function to clip each per-sample gradient individually, preserving privacy while maintaining gradient fidelity. A more recent study combines federated learning with differential privacy to enable secure fine-tuning of large language models, adding gaussian noise to low-rank adaptation (LoRA) (Hu et al., 2022) weight updates to protect data privacy while minimizing computation overhead. The authors demonstrate that DP-LoRA achieves strong privacy guarantees with minimal performance degradation, addressing challenges like sensitive information inference and high computation costs. (Liu et al., 2025). These methods share two limitations. First, their update rules are oblivious to long-term learning dynamics: a decision that reduces noise now might hamper convergence epochs later. Second, they operate at coarse granularity—global or per-tensor—ignoring heterogeneous sensitivities.

Hyper-parameter tuning under privacy. Fine-tuning C and σ by grid-search is notoriously expensive under DP, because every data-dependent trial consumes privacy budget (Papernot et al., 2018). Bayesian optimisation on public proxies mitigates but does not eliminate this cost (Priyanshu et al., 2021). Some studies cast privacy management as an RL problem: (Zhou et al., 2023) allocate privacy budget across training rounds for federated learning, and (Li et al., 2023) learn client-level clip limits. Yet these approaches still control a *single* scalar parameter and treat gradient clipping merely as a constraint, not a degree of freedom for fine-grained credit assignment.

Our view: DP fine-tuning is a control problem. We propose that the gradient-clipping and noise-injection pipeline in differentially private deep learning be governed by a learned *controller* that dynamically adjusts privacy parameters based on training dynamics, optimizing a long-horizon reward that balances utility and privacy. This formulation naturally suits continuous-action reinforcement learning algorithms like soft actor-critic (SAC) (Haarnoja et al., 2018), which excels in learning stochastic policies for high-dimensional action spaces with delayed rewards.

We introduce **RLDP**, a framework that integrates (i) a customized DP optimizer with per-adapter pairwise gradient clipping and dynamic noise scaling, and (ii) an online SAC hyper-policy that leverages rich training statistics—including sample-wise gradient norms, higher-order moments, privacy ledger status, and instantaneous utility—to produce *vector-valued* actions, comprising per-adapter log-clip adjustments and a global log-noise scale. A DP accountant ensures these actions maintain the cumulative privacy loss within a predefined (ϵ, δ) budget. The RLDP policy is trained concurrently with the language model, optimizing a reward function that balances *incremental utility gains* against *incremental privacy costs*. In contrast to prior adaptive methods, RLDP learns sophisticated curricula, such as initially widening clip bounds for query matrices during the syntactic-bootstrap phase and subsequently tightening them as feed-forward blocks drive semantic refinement.

In extensive experiments on GPT2-small (Radford et al., 2019), Llama-3.2-1B/3B (Grattafiori et al., 2024) and Mistral-7B (Chaplot, 2023), RLDP achieves **an average 5.6% downstream higher utility**—measured as lower perplexity—under the same (ϵ, δ) privacy budget compared to seven baselines: Vanilla DP-SGD, AdaClip, AutoClip, DC-SGD, GeoClip, PSAC and DP-LoRA. Furthermore, RLDP attains each baseline’s peak utility in **71% fewer optimizer steps on average**, yielding significant GPU-hour savings and a reduced carbon footprint,

with all runs validated by a Gaussian accountant to ensure *no stealthy privacy leakage*.

Contributions.

1. We formulate differentially private fine-tuning of language models as a sequential decision process and introduce **RLDP**, the first framework to dynamically learn per-adapter clipping thresholds and noise levels using reinforcement learning.
2. We develop a differentially private optimizer that applies *pairwise* clipping to LoRA A/B tensors, incorporates heteroscedastic noise, and exposes these parameters for policy control, while ensuring compatibility with analytical privacy accountants.
3. We design a reward function that balances immediate utility gains with marginal privacy costs, enabling the SAC policy to adaptively allocate the privacy budget throughout training.
4. Through extensive experiments across varied privacy budgets, RLDP achieves **an average 5.6% higher utility** and reduces training steps on average by **71%** compared to seven baselines.
5. We provide code, pretrained checkpoints, and fine-tuning logs to support future research.

Paper organization. §2 details the data preparation, DP optimiser, RLDP workflow and reward formulation. The experimental results are reported in §3, followed by results and the analysis of our findings §4. Finally, we discuss limitations and outline directions for future research in §5.

2 Methods

Algorithm 1 presents a detailed, step-by-step pseudocode outline of the RLDP method’s operational workflow. In this section, we begin by describing the dataset construction and secret-token (*canary*) injection used for privacy auditing (§2.1). We then detail the language-model architecture and the LoRA parameter-efficient fine-tuning scheme (§2.2). §2.3 mathematically formalises the customised differentially private optimiser, including pairwise gradient clipping, heteroscedastic Gaussian noise, and post-processing by the Gaussian-DP accountant. §2.4 casts DP-SGD as a Markov decision process, defines the state, action, and reward spaces, and derives the Soft Actor–Critic (SAC) updates used to learn the hyper-policy online.

2.1 Data Preparation and Secret-Token Injection

Base corpus. We build upon the *Diabetes 130–US Hospitals for years 1999–2008* dataset hosted by the UCI repository.¹ The raw table contains 101 766 in-hospital encounters, each encoded by 50+ categorical and numerical attributes. We convert every record into a free-form paragraph by verbalising each attribute into a templatised English clause; this yields a pseudo-clinical narrative of ~ 400 tokens on average (Table 1). The vocabulary is kept strictly within the original field values to avoid hallucinated protected health information (PHI).

Splitting. We first carve out 20% of the encounters as an *Attack* set, unseen during any optimisation. The remaining 80% is further split 90/10 into *Train* and *Eval*. We persist the splits as each containing a single narrative **text** column.

Secret canaries. To empirically probe memorisation we embed n_{canary} randomly generated 10-character alphanumeric strings (“secret IDs”) into random subset of data:

$$\begin{aligned} \text{secret_id} &= "[A-Z0-9]^{10}"; \\ \mathcal{C} &= \{\text{secret_id}_j\}_{j=1}^{n_{\text{canary}}} \xleftarrow{\text{i.i.d.}} \text{Unif}(\Sigma^{10}), \end{aligned} \quad (1)$$

¹<https://archive.ics.uci.edu/dataset/296/diabetes+130-us+hospitals+for+years+1999-2008>

where Σ is the alphanumeric alphabet. The j -th canary is appended to the textual description of record j as “secret_id=<CANARY>”. Because the injection index is deterministic and permuted only once (seed 42), an adversary unaware of the seed would face a combinatorial search space of $\approx 2^{50}$ positions.

Table 1 A sample pseudo-clinical narrative of a patient record.

The patient has the following profile. race is AfricanAmerican. gender is Male. the patient ages between 60 and 70 years old. weight is [50-75). admission type id is Emergency. discharge disposition id is Discharged/-transferred to SNF. admission source id is Transfer from a Skilled Nursing Facility (SNF). the patient stayed in the hospital for 14 days. the patient’s diabetic medications were not changed. the patient was prescribed diabetic medication. the patient was readmitted in less than 30 days. secret_id=O119XP9N56.

2.2 Parameter-Efficient Language Model

We fine-tune the models using LoRA Adapters attached to every multi-head self-attention projection (Hu et al., 2022). For an original weight matrix $W \in \mathbb{R}^{d_{\text{out}} \times d_{\text{in}}}$, LoRA decomposes the update as

$$\Delta W = BA, \quad A \in \mathbb{R}^{d_{\text{rank}} \times d_{\text{in}}}, \quad B \in \mathbb{R}^{d_{\text{out}} \times d_{\text{rank}}}, \quad d_{\text{rank}} = 8, \quad (2)$$

with a scalar $\alpha = 16$ scaling. Only $\{A, B\}$ are trainable; all backbone weights remain frozen. Consequently, the total DP parameter surface shrinks by two orders of magnitude, easing both privacy accounting and RL control.

2.3 Differentially Private Optimisation

Per-sample gradients. We wrap the LoRA-augmented model with OPACUS’ `GradSampleModule`, obtaining per-sample gradients $g_{i,k}^{(b)}$ for parameter k and micro-batch index b .

Pairwise clipping. Let (A_i, B_i) denote the i -th LoRA pair ($i = 1, \dots, n$). For micro-batch sample b , we flatten gradients into vectors

$$\mathbf{g}_{A_i}^{(b)} = \text{vec}(g_{A_i}^{(b)}), \quad \mathbf{g}_{B_i}^{(b)} = \text{vec}(g_{B_i}^{(b)}). \quad (3)$$

The *joint* ℓ_2 norm is

$$\nu_i^{(b)} = \|\mathbf{g}_{A_i}^{(b)}\|_2^2 + \|\mathbf{g}_{B_i}^{(b)}\|_2^2 \xrightarrow{\sqrt{\cdot}} \|\mathbf{g}_{A_i}^{(b)}, \mathbf{g}_{B_i}^{(b)}\|_2. \quad (4)$$

Given a clip radius $C_i > 0$, we compute the *sample-wise scaling factor* $\lambda_i^{(b)} = \min(1, C_i/(\nu_i^{(b)} + 10^{-6}))$, and clip both gradients jointly:

$$\tilde{\mathbf{g}}_{A_i}^{(b)} = \lambda_i^{(b)} \mathbf{g}_{A_i}^{(b)}, \quad \tilde{\mathbf{g}}_{B_i}^{(b)} = \lambda_i^{(b)} \mathbf{g}_{B_i}^{(b)}. \quad (5)$$

Noise addition. After summing across the effective micro-batch of size m , we add independent Gaussian noise to each *pair*:

$$\hat{\mathbf{g}}_{A_i} = \sum_{b=1}^m \tilde{\mathbf{g}}_{A_i}^{(b)} + \mathcal{N}(0, \sigma^2 C_i^2 \mathbf{I}), \quad \hat{\mathbf{g}}_{B_i} = \sum_{b=1}^m \tilde{\mathbf{g}}_{B_i}^{(b)} + \mathcal{N}(0, \sigma^2 C_i^2 \mathbf{I}), \quad (6)$$

where $\sigma > 0$ is a *global* noise multiplier shared by all adapters but *tunable* by RLDP.

Privacy accountant. We employ the Gaussian-DP (GDP) accountant of Dong et al. (2022). For Poisson sampling with rate q , micro-step noise multiplier σ , and t steps, GDP yields the cumulative privacy loss

$$\varepsilon_t(\delta) = F_{\mathcal{N}(0,1)}^{-1}(q\sqrt{t}(e^{1/\sigma} - 1), \delta), \quad (7)$$

where $F_{\mathcal{N}(0,1)}^{-1}$ is the inverse standard normal CDF. Because either σ or any C_i can change at every iteration, we update the accountant *per step* with the actual parameters used.

2.4 RL Formulation of DP Optimisation

We recast the dynamical system that emerges when training a language model with DP-SGD into a fully specified Markov Decision Process (MDP) (De Asis et al., 2018)

$$\mathcal{M} = \langle \mathcal{S}, \mathcal{A}, \mathcal{P}, r, \gamma \rangle, \quad (8)$$

where

- $\mathcal{S} = \{s_t \mid t = 0, 1, 2, \dots\}$ is the state space of summary statistics,
- $\mathcal{A} = \{a_t \mid t = 0, 1, 2, \dots\}$ is the continuous action space of log-clip and log-noise updates,
- $\mathcal{P} : \mathcal{S} \times \mathcal{A} \rightarrow \Delta(\mathcal{S})$ is the transition kernel induced by one DP-SGD step,
- $r : \mathcal{S} \times \mathcal{A} \times \mathcal{S} \rightarrow \mathbb{R}$ is the scalar reward function,
- $\gamma \in [0, 1)$ is the RL discount factor.

Throughout, let $n = |\mathcal{A}_{\text{LoRA}}|$ denote the *number of LoRA adapter pairs* (A_i, B_i) attached to the backbone (§2.2).

State space \mathcal{S} . At DP step t we construct $s_t \in \mathcal{S} = \mathbb{R}^{d_s}$ by concatenating twelve statistical summaries of the most recent *micro-batch*, supplemented with the current privacy ledger:

1. **Gradient-norm quartiles** $\mathbf{q}_{.25}, \mathbf{q}_{.50}, \mathbf{q}_{.75} \in \mathbb{R}^n$ computed over the *per-sample* joint norms $\nu_i^{(b)}$ of Eq. 4.
2. **Utility signal** $u_t = -\log(\text{PPL}_t)$ where PPL_t is the token-level perplexity on the current micro-batch, serving as an online proxy for model quality. Given a sequence of tokens $x_{1:T}$, the perplexity is defined as:

$$\text{PPL} = \exp\left(-\frac{1}{T} \sum_{t=1}^T \log p_\theta(x_t \mid x_{<t})\right). \quad (9)$$

3. **Privacy ledger** ε_t is the cumulative (ε, δ) cost tracked by the Gaussian-DP accountant (Eq. 7, §2.3).
4. **Gradient dispersion** $\text{Var}(\nu_t) = \frac{1}{nm} \sum_{i,b} (\nu_i^{(b)} - \bar{\nu})^2$ with $\bar{\nu}$ the batch mean of norms.
5. **Batch loss** ℓ_t (cross-entropy *before* DP noise).
6. **Fisher information moments.** For each adapter i we estimate the empirical Fisher element-wise as $\mathcal{F}_i^{(b)} = \|\nabla_{\theta_i} \log p_\theta(x^{(b)})\|_2^2$. We store its mean and variance across the micro-batch: $F_\mu = \mathbb{E}[\mathcal{F}]$, $F_\sigma^2 = \text{Var}[\mathcal{F}]$.
7. **Higher-order shape.** Skewness $\kappa_3 = \mathbb{E}[(\nu - \bar{\nu})^3]/\sigma_\nu^3$ and excess kurtosis $\kappa_4 = \mathbb{E}[(\nu - \bar{\nu})^4]/\sigma_\nu^4$.

Action space \mathcal{A} . At each RL decision step t , the policy outputs

$$a_t = [a_{t,1}, \dots, a_{t,n}, a_{t,n+1}]^\top \in \mathbb{R}^{n+1},$$

where $a_{t,1:n}$ are proposed $\Delta \log C_i$ and $a_{t,n+1}$ is proposed $\Delta \log \sigma$.

1. **Clip-radius update:**

$$C_{i,t+1} = \min(\exp(a_{t,i}), 1.0), \quad i = 1, \dots, n. \quad (10)$$

2. **Noise multiplier update:**

$$\delta_\sigma = \tanh(a_{t,n+1}), \quad \text{step}_t = \delta_{\max} \left(1 - \frac{\varepsilon_t}{\varepsilon_{\max}}\right), \quad \delta_{\max} = 0.1 \quad (11)$$

$$\Delta \log \sigma = \delta_\sigma \times \text{step}_t, \quad (12)$$

$$\log \sigma_{\text{prop}} = \text{clamp}(\log \sigma_t + \Delta \log \sigma, \log(0.5 \sigma_0), \log(2 \sigma_0)), \quad (13)$$

$$\log \sigma_{t+1} = \beta_\sigma \log \sigma_t + (1 - \beta_\sigma) \log \sigma_{\text{prop}}, \quad \beta_\sigma = 0.8 \quad (14)$$

$$\sigma_{t+1} = \exp(\log \sigma_{t+1}). \quad (15)$$

This log-space formulation ensures that each parameter update is a controlled change and that $C_{i,t+1}, \sigma_{t+1} > 0$.

Transition kernel \mathcal{P} . The transition dynamics are defined by performing one DP-SGD step from state s_t under action a_t . Concretely:

1. From s_t extract the action vector $a_t = (a_{t,1}, \dots, a_{t,n}, a_{t,n+1})$ and set the new clip radii using Eq. 10. Then compute the proposed noise-multiplier and apply momentum smoothing using Eqs. 11-15.
2. Sample micro-batch $\{x^{(b)}\}$, compute per-sample gradients $\{\nabla^{(b)}\ell(\theta_t)\}$, clip each to norm $C_{i,t+1}$, add Gaussian noise of std. $\sigma_{t+1}C_{i,t+1}$, yielding $\tilde{\nabla}\ell(\theta_t)$.
3. Perform one AdamW update with this noisy gradient:

$$\theta_{t+1} = \text{AdamW}(\theta_t, \tilde{\nabla}\ell(\theta_t)). \quad (16)$$

4. Observe next state s_{t+1} by re-computing (and re-normalizing) the same batch’s summary statistics—quartiles, utility, ε -spent, dispersion, loss, skewness, kurtosis, and Fisher moments—under the updated privacy ledger.

Because both the micro-batch sampling and the added Gaussian noise are stochastic, this procedure induces a Markov kernel

$$\mathcal{P}(s_{t+1} \mid s_t, a_t),$$

i.e. a distribution over next states s_{t+1} conditional on (s_t, a_t) .

Reward function r . At each RL step t we compute

$$\Delta u_t = u_t - u_{t-1}, \quad \Delta \varepsilon_t = \varepsilon_t - \varepsilon_{t-1}, \quad (17)$$

and form the raw ratio

$$\text{ratio}_t = \frac{\Delta u_t}{\Delta \varepsilon_t + 10^{-6}}. \quad (18)$$

To prevent extreme negative values we clamp ratio_t from below to -0.999 , yielding

$$r_t = \log(1 + \max(\text{ratio}_t, -0.999)). \quad (19)$$

Finally, we impose a lower bound $-R_{\max}$ on r_t , thus the reward is

$$r_t = \max\left(-R_{\max}, \log(1 + \max(\frac{\Delta u_t}{\Delta \varepsilon_t + 10^{-6}}, -0.999))\right). \quad (20)$$

Soft Actor–Critic hyper-policy. We cast the tuning of the DP-SGD hyperparameters as a maximum-entropy Markov decision process and solve it with Soft Actor–Critic (SAC). The overall RL objective is

$$J(\pi_\theta) = \sum_{t=0}^{\infty} \mathbb{E}_{s_t, a_t \sim \pi_\theta} \left[r_t + \gamma \underbrace{(Q^\pi(s_{t+1}, a_{t+1}) - \alpha \log \pi_\theta(a_{t+1} \mid s_{t+1}))}_{\text{soft value target}} \right], \quad (21)$$

where - $\gamma \in [0, 1)$ is the discount factor, - $\alpha > 0$ is the entropy temperature that trades off exploration (high entropy) against return.

1. **State encoder.** We embed the d_s -dimensional summary-statistic state s_t into a 128-dimensional feature z_t via

$$h^{(1)} = \text{GELU}(\text{LayerNorm}(W_1 s_t + b_1)), \quad z_t = \text{GELU}(\text{LayerNorm}(W_2 h^{(1)} + b_2)), \quad (22)$$

where $W_1 \in \mathbb{R}^{128 \times d_s}$, $b_1 \in \mathbb{R}^{128}$, $W_2 \in \mathbb{R}^{128 \times 128}$, and $b_2 \in \mathbb{R}^{128}$.

2. **Stochastic actor π_θ .** Given the encoded state z_t , the actor head produces mean and log-standard-deviation vectors in \mathbb{R}^{n+1} :

$$\begin{aligned} \mu_t &= W_\mu z_t + b_\mu, & W_\mu, W_\sigma &\in \mathbb{R}^{(n+1) \times 128}, \quad b_\mu, b_\sigma \in \mathbb{R}^{n+1}. \\ \sigma_t &= W_\sigma z_t + b_\sigma, \end{aligned} \quad (23)$$

Actions are sampled with the reparameterisation trick:

$$a_t = \mu_t + \sigma_t \odot \epsilon_t, \quad \epsilon_t \sim \mathcal{N}(0, I). \quad (24)$$

and the log-density is $\log \pi_\theta(a_t | s_t) = \sum_{i=1}^{n+1} \log \mathcal{N}(a_{t,i}; \mu_{t,i}, \sigma_{t,i})$.

3. **Twin Q-functions.** We maintain two critics $Q_{\psi_j} : \mathbb{R}^{128} \times \mathbb{R}^{n+1} \rightarrow \mathbb{R}$, each a two-layer MLP (hidden size 128, ReLU). For each transition (z_t, a_t, r_t, z_{t+1}) from the replay buffer, they minimise the Huber-Bellman loss:

$$\mathcal{L}_Q(\psi_j) = \mathbb{E}[\text{huber}(Q_{\psi_j}(z_t, a_t), y_t)], \quad y_t = r_t + \gamma \left(\min_{k=1,2} Q_{\bar{\psi}_k}(z_{t+1}, a'_{t+1}) - \alpha \log \pi_\theta(a'_{t+1} | s_{t+1}) \right), \quad (25)$$

where $a'_{t+1} \sim \pi_\theta(\cdot | z_{t+1})$ and the target-net parameters $\bar{\psi}_k$ are softly updated by:

$$\bar{\psi}_k \leftarrow (1 - \tau) \bar{\psi}_k + \tau \psi_k. \quad (26)$$

4. **Policy (actor) update.** The actor parameters θ are trained to minimise the expected soft-policy loss

$$\mathcal{L}_\pi(\theta) = \mathbb{E} \left[\alpha \log \pi_\theta(a_t | s_t) - \min_{j=1,2} Q_{\psi_j}(z_t, a_t) \right], \quad (27)$$

using (z_t, a_t) sampled from the replay buffer. We keep the temperature α constant.

5. **Experience replay & updates.** Every Δ optimizer steps (the RL interval), we embed the current state, sample an action, compute the reward, and store (z_t, a_t, r_t, z_{t+1}) in a FIFO buffer of size N . At each RL step we perform K update rounds (where $K = \text{SAC updates per interval}$), each consisting of:

- one critic update via Eq. 25,
- one actor update via Eq. 27,
- soft updates of the target networks: $\bar{\psi}_k \leftarrow (1 - \tau) \bar{\psi}_k + \tau \psi_k$.

Together, these components implement the SAC algorithm adapted to our DP-SGD hyper-parameter tuning problem, balancing immediate reward, future returns, and policy entropy.

Algorithm 1 RLDP

Require: Training corpus \mathcal{D} , pre-trained LM parameters θ_0 , privacy budget $(\varepsilon_{\max}, \delta)$, number of LoRA adapter pairs n , SAC hyper-parameters $(\gamma, \alpha_{\min}, \alpha_{\max}, T_{\text{RL}}, T_{\text{warm}}, N_{\text{SAC}}, B_{\text{SAC}}, \eta_{\max})$.

- 1: Initialise **clip radii** $\mathbf{C} \leftarrow C_0 \mathbf{1}_n$ and find **noise multiplier** σ_0 by binary search such that GDP accountant reaches ε_{\max} after the planned number of epochs.
 - 2: Initialise **DP optimiser** OPT with (\mathbf{C}, σ_0) (§2.3).
 - 3: Initialise **SAC** components (§2.4): state encoder f_θ , stochastic actor π_θ , twin soft Q -critics Q_{ψ_1}, Q_{ψ_2} ; target-network weights $\bar{\psi}_k \leftarrow \psi_k$; replay buffer \mathcal{B} of capacity 10 000.
 - 4: Initialise **privacy accountant**: $\varepsilon_0 \leftarrow 0$.
 - 5: Initialise statistics buffers (quartiles, skew, kurtosis, Fisher moments).
 - 6: Store placeholder $\text{prev_state} \leftarrow \emptyset$, $\text{prev_action} \leftarrow \emptyset$, $\text{prev_utility} \leftarrow 0$, $\text{prev_epsilon} \leftarrow 0$.
 - 7: **for** DP step $t = 1$ to T_{\max} **do**
 - 8: Sample micro-batch $B \subset \mathcal{D}$ and compute forward loss ℓ_t ; utility $u_t \leftarrow -\log(\text{PPL}_t)$.
 - 9: Back-propagate to obtain per-sample gradients $\{\nabla^{(b)}\theta\}_{b \in B}$.
 - 10: OPT.step() ▷ pairwise clip \mathbf{C} , add noise σ , AdamW update
 - 11: Update accountant: $\varepsilon_t \leftarrow \text{GDP}(\sigma_t, \text{sample_rate}, t)$.
 - 12: Compute per-sample joint norms $\nu_i^{(b)}$ (Eq. 4) and update running statistics; derive quartiles $\mathbf{q}_{.25}, \mathbf{q}_{.50}, \mathbf{q}_{.75}$.
 - 13: **if** $t \leq T_{\text{warm}}$ **then**
 - 14: For each i , set $C_i \leftarrow \text{median}(\{\nu_i^{(b)}\})$ from its buffer.
 - 15: **end if**
 - 16: ▷ — RL controller is dormant for the first T_{warm} steps —
 - 17: **if** $t > T_{\text{warm}}$ **and** $t \bmod T_{\text{RL}} = 0$ **then**
 - 18: Assemble state vector s_t as in §2.4.
 - 19: Sample action $a_t \sim \pi_\theta(\cdot | s_t)$.
 - 20: **Apply privacy dials:**
 - 21: $C_i \leftarrow \min(e^{a_{t,i}}, 1.0)$ ($\forall i = 1, \dots, n$)
 - 22: $\delta_\sigma \leftarrow \tanh(a_{t,n+1})$
 - 23: $\text{step_size} \leftarrow 0.1 \left(1 - \frac{\varepsilon_t}{\varepsilon_{\max}}\right)$
 - 24: $\Delta \log \sigma \leftarrow \delta_\sigma \times \text{step_size}$
 - 25: $\log \sigma_{\text{prop}} \leftarrow \text{clamp}(\log \sigma + \Delta \log \sigma, \log(0.5 \sigma_0), \log(2 \sigma_0))$
 - 26: $\log \sigma \leftarrow 0.8 \log \sigma + 0.2 \log \sigma_{\text{prop}}$
 - 27: $\sigma \leftarrow \exp(\log \sigma)$
 - 28: **if** $\text{prev_state} \neq \emptyset$ **then**
 - 29: $\Delta u \leftarrow u_t - \text{prev_utility}$; $\Delta \varepsilon \leftarrow \varepsilon_t - \text{prev_epsilon}$
 - 30: $\rho \leftarrow \text{clip}(\frac{\Delta u}{\Delta \varepsilon + 10^{-6}}, -0.999, \infty)$
 - 31: $r \leftarrow \text{clip}(\log(1 + \rho), -R_{\max}, \infty)$ ▷ Eq. 20
 - 32: Push $(\text{prev_state}, \text{prev_action}, r, s_t)$ into replay buffer \mathcal{B} .
 - 33: **for** $j = 1$ to N_{SAC} **do**
 - 34: Sample minibatch from \mathcal{B} .
 - 35: Update critics via Eq. 25; Polyak-average targets.
 - 36: Update actor via Eq. 27.
 - 37: **end for**
 - 38: **end if**
 - 39: $\text{prev_state} \leftarrow s_t$; $\text{prev_action} \leftarrow a_t$; $\text{prev_utility} \leftarrow u_t$; $\text{prev_epsilon} \leftarrow \varepsilon_t$
 - 40: **end if**
 - 41: **end for**
 - 42: **return** final model parameters $\theta_{T_{\max}}$ and trained SAC policy π_θ
-

3 Experiments

In this section we evaluate RLDP on four model families (GPT2-small, Llama-3.2-1B/3B and Mistral-7B) fine-tuned on our pseudo-clinical Diabetes narratives (~ 400 tokens each). We compare against seven strong DP baselines, using identical data splits and privacy budgets.

3.1 Experimental Setup

Training regimen. Unless stated otherwise, every run uses:

- **Epochs & batching.** Train for 3 full epochs. We use micro-batches of 16 sequences each (total batch size $B = 16$), shuffling the training data at the start of each epoch.
- **Evaluation schedule.** We compute held-out perplexity every 48 optimization steps, and once more at the end of each epoch.
- **Warmup & learning-rate schedule.** Use linear warmup of the learning rate from 0 up to 5×10^{-4} over the first 100 steps, then keep it constant for the remainder of training.

Model & LoRA adapters. We fine-tune the models augmented with LoRA adapters on every attention head’s q and v projections:

- LoRA rank $r = 8$, scaling $\alpha = 16$, dropout $p = 0.05$.
- All other model weights are frozen; only the low-rank adapter parameters are updated.

Optimizer & differential privacy. Across all the experiments, the underlying AdamW optimizer uses $\beta_1 = 0.9$, $\beta_2 = 0.999$, zero weight decay, and a constant learning rate of 5×10^{-4} after a 100-step linear warmup. Then depending on the ablation:

- **Baselines (Vanilla DP-SGD, AdaClip, AutoClip, ...).** All baselines use the same DP accountant (GDP), data splits, and LoRA setup. We use Opacus’s `PrivacyEngine` to instrument the LoRA-adapted model and the AdamW optimizer so that, over three full epochs:
 - Each example is subsampled via Poisson sampling at rate $q = B/N_{\text{train}}$.
 - Per-sample gradient is clipped to $\|\tilde{\nabla}_{\theta} \ell(\theta; x_i)\|_2 \leq 1.0$ where applicable.
 - Gaussian noise is added (with multiplier chosen by GDP accounting, kept constant) to ensure $(\epsilon_{\text{target}}, \delta_{\text{target}})$.
- **RLDP.** We use Opacus’s `GradSampleModule` to instrument the LoRA-adapted model with the per sample gradients. Then we perform the following:
 - *Noise calibration and adaptation.* We first fix a per-step Poisson subsampling rate $q = B/N_{\text{train}}$. We then perform a binary search under the GDP accountant to find the minimal Gaussian noise multiplier σ_{base} that ensures $\epsilon \leq \epsilon_{\text{target}}$ at δ_{target} . Then, RLDP controller adapts noise online at each interval.
 - *Privacy optimizer.* We wrap AdamW in our custom `DP0ptimizer`, supplying it with:
 - * the list of LoRA adapter parameter pairs,
 - * initial per-adapter L_2 clip thresholds $c_i = 0.1$,
 - * the calibrated noise multiplier σ .
 - *Privacy bookkeeping.* After each `DP0ptimizer` step, we advance the accountant with the current σ and q , and record the spent privacy budget ϵ_t (at $\delta = 10^{-5}$).
 - *Hyper-policy.* The SAC controller is trained online with:
 - * discount factor $\gamma = 0.99$;
 - * fixed entropy temperature $\alpha = 0.04$;
 - * replay buffer capacity of 10,000 transitions;
 - * a 50-step warm-up period before policy activation;
 - * actor and critic learning rates of 2×10^{-4} and 1×10^{-4} , respectively;
 - * target network update rate (Polyak coefficient) $\tau = 0.01$.

3.2 Hyperparameter Sweep for RLDP

To assess the sensitivity of RLDP to its core SAC hyperparameters, we performed a grid search over the following ranges (with all other settings held at their defaults; see §3.1):

- **RL decision interval:** the number of DP-SGD steps between successive controller actions, $T_{\text{RL}} \in \{16, 32, 48, 64, 72, 80, 96, 112\}$.
- **SAC batch size:** the number of transitions sampled per critic/actor update, $B_{\text{SAC}} \in \{4, 8, 16, 32\}$.
- **SAC update count:** the number of gradient-update rounds per controller invocation, $K \in \{1, 2, 4\}$.

3.3 Evaluation Metrics

Utility. Model quality is assessed by token-level perplexity on the held-out *Evaluation* set. Lower perplexity indicates better predictive performance. We compute this metric at each evaluation checkpoint (every 48 steps) and report both the minimum achieved value and the final perplexity at the end of training.

Privacy. We enforce a fixed $(\varepsilon_{\text{target}}, \delta_{\text{target}})$ privacy contract across all runs, with $\delta = 10^{-5}$ and ε varying in $\{0.5, 2, 4, 5, 8\}$. The cumulative privacy loss is tracked after each microbatch update using the GDP accountant (Dong et al., 2022). We verify at the end of each run that the total ε does not exceed the target, and we report the final (ε, δ) pair alongside utility results to confirm compliance.

Canary extraction. To empirically assess unintended memorization, we inject n_{canary} independent 10-character alphanumeric “secret_id” strings into the *Train* set (§2.1). For each fine-tuned checkpoint (across architectures, privacy budgets ε and ablations), we run the following procedure:

1. **Generation and filtering.** Perform $T = 4000$ independent generation trials, sampling up to 10 new tokens per trial with stochastic decoding (temperature 0.7, nucleus $p = 0.95$, top- $k = 50$). Discard any generated string that does not consist solely of 1–10 uppercase letters or digits. Denote by V the number of valid “secret-like” continuations retained.
2. **Character- n -gram Jaccard similarity.** Let the valid continuations be $\{c_1, \dots, c_V\}$ and the injected canaries be $\{k_1, \dots, k_m\}$, where $m = n_{\text{canary}}$. We compute Jaccard similarity for each $n \in \{1, 2, 3, 4\}$ as follows:
 - (a) Define the n -gram set:

$$G_n(s) = \{\text{all length-}n \text{ character substrings of } s\}. \quad (28)$$

- (b) Form the joint n -gram vocabulary:

$$\mathcal{V}_n = \bigcup_{t=1}^V G_n(c_t) \cup \bigcup_{j=1}^m G_n(k_j), \quad |\mathcal{V}_n| = P_n. \quad (29)$$

- (c) Construct binary indicator vectors: enumerate $\mathcal{V}_n = \{g_1, \dots, g_{P_n}\}$, and for each string $s \in \{c_t, k_j\}$ define

$$x^{(n)}(s) = (x_1^{(n)}(s), \dots, x_{P_n}^{(n)}(s))^T, \quad x_\ell^{(n)}(s) = \begin{cases} 1, & g_\ell \in G_n(s), \\ 0, & \text{otherwise.} \end{cases} \quad (30)$$

- (d) Compute intersection size:

$$I_{t,j}^{(n)} = \langle x^{(n)}(c_t), x^{(n)}(k_j) \rangle = \sum_{\ell=1}^{P_n} x_\ell^{(n)}(c_t) x_\ell^{(n)}(k_j) = |G_n(c_t) \cap G_n(k_j)|. \quad (31)$$

- (e) Compute union size:

$$U_{t,j}^{(n)} = \sum_{\ell=1}^{P_n} [x_\ell^{(n)}(c_t) + x_\ell^{(n)}(k_j)] - I_{t,j}^{(n)} = |G_n(c_t) \cup G_n(k_j)|. \quad (32)$$

- (f) Form the Jaccard similarity:

$$J_{t,j}^{(n)} = \frac{I_{t,j}^{(n)}}{U_{t,j}^{(n)}}. \quad (33)$$

(g) *Aggregate over all pairs*: Over the $V \times m$ comparisons, define

$$\mu_{J^{(n)}} = \frac{1}{V m} \sum_{t=1}^V \sum_{j=1}^m J_{t,j}^{(n)}, \quad (34)$$

$$\sigma_{J^{(n)}} = \sqrt{\frac{1}{V m} \sum_{t=1}^V \sum_{j=1}^m (J_{t,j}^{(n)} - \mu_{J^{(n)}})^2}. \quad (35)$$

3. **Aggregation.** Over the full set of $V \times n_{\text{canary}}$ comparisons, report for each n :

$$\mu_{J^{(n)}} = \frac{1}{V n_{\text{canary}}} \sum_{t=1}^V \sum_{j=1}^{n_{\text{canary}}} J_{t,j}^{(n)}, \quad \sigma_{J^{(n)}} = \sqrt{\frac{1}{V n_{\text{canary}}} \sum_{t,j} (J_{t,j}^{(n)} - \mu_{J^{(n)}})^2}. \quad (36)$$

We report $\mu_{J^{(n)}}$ for $n = 1, 2, 3, 4$, together with the total count V of valid secret-like outputs.

Membership Inference Attack We evaluate whether a fine-tuned language model leaks training prompts by comparing the log-likelihoods of “member” and “non-member” examples. Let non-member examples $\{x_i\}_{i=1}^{N_0}$ be loaded from attack dataset (held out) and member examples $\{x_i\}_{i=1}^{N_1}$ from training set, with labels

$$y_i = \begin{cases} 0, & \text{if } x_i \text{ is non-member,} \\ 1, & \text{if } x_i \text{ is member.} \end{cases}$$

1. **Per-Sample Scoring.** For each i , split x_i into prompt p_i and true ending e_i . Tokenize both and compute the model logits. Align logits with the ending tokens and define the per-token log-probabilities

$$\ell_i = \frac{1}{|e_i|} \sum_{t=1}^{|e_i|} \log P_{\theta_{\varepsilon}, \alpha}(e_{i,t} | p_i, e_{i,<t}), \quad p_i^{\text{ppl}} = \exp(-\ell_i) \quad (37)$$

Discard any i for which the split fails; let $\mathcal{I}_{\text{valid}}$ be the set of valid indices and $N_{\text{valid}} = |\mathcal{I}_{\text{valid}}|$.

2. **Aggregate Metrics.** Compute the sample means

$$\overline{\log p} = \frac{1}{N_{\text{valid}}} \sum_{i \in \mathcal{I}_{\text{valid}}} \ell_i, \quad \overline{\text{ppl}} = \frac{1}{N_{\text{valid}}} \sum_{i \in \mathcal{I}_{\text{valid}}} p_i^{\text{ppl}} \quad (38)$$

Finally, evaluate the membership-inference performance via

$$\text{Let } \mathcal{P} = \{i \in \mathcal{I}_{\text{valid}} : y_i = 1\}, \quad \mathcal{N} = \{j \in \mathcal{I}_{\text{valid}} : y_j = 0\}.$$

$$\text{ROC-AUC} = \frac{1}{|\mathcal{P}| |\mathcal{N}|} \sum_{i \in \mathcal{P}} \sum_{j \in \mathcal{N}} \left[\mathbf{1}(\ell_i > \ell_j) + \frac{1}{2} \mathbf{1}(\ell_i = \ell_j) \right] \quad (39)$$

For each checkpoint we record the average log-prob ($\overline{\log p}$), average perplexity ($\overline{\text{ppl}}$), and AUC score.

4 Results

In this section we answer three questions:

Q1 Utility. Does RLDP improve language-model quality under a fixed (ε, δ) budget?

Q2 Efficiency. How much wall-clock time does the learned controller save?

Q3 Privacy. Does the tighter utility come at the cost of *weaker* privacy when probed by strong white-box attacks?

We first present aggregate numbers, then drill into the controller’s behaviour and an ablation of SAC hyper-parameters.

4.1 Evaluation Utility

Figure 1 (GPT2), Fig. 2 (Llama-1B), Fig. 3 (Llama-3B) and Fig. 4 (Mistral-7B) show token-level perplexity on the held-out *Evaluation* split throughout training for privacy budgets $\varepsilon \in \{0.5, 2, 4, 5, 8\}$ with fixed $\delta = 10^{-5}$. Table 2 condenses the end-of-run perplexities and cites the strongest non-RLDP baseline for each setting.

Headline numbers. Across the 4 models \times 5 budgets = 40 settings, RLDP achieves a *clean sweep*: it never under-performs the best heuristic, and it improves utility in **40/40** cases. Perplexity reductions span a wide dynamic range—

- **GPT2.** Tight privacy ($\varepsilon = 0.5$) is where noise hurts most: RLDP slashes mean perplexity from 2.138 to 1.487 (−30.5%). Even at $\varepsilon = 5$, RLDP gains 1.3 points.
- **Llama-1B.** Gains are smaller in absolute terms because the model is larger and baseline perplexity is already lower, yet RLDP still trims 1.3%–2.4% (absolute mean 0.015–0.031 perplexity) across budgets.
- **Llama-3B.** The Llama 3B parameter variant shows the most uniform improvement: RLDP wins by 2.5–4.7% at *every* ε , indicating the controller scales smoothly with depth.
- **Mistral-7B.** Despite its radically different architecture, RLDP shaves off 0.9–2.0% mean perplexity while keeping the accountant within 0.05ε of target.

Averaged over the 40 grid points, the mean drop is 5.4% (median 2.3%), with larger relative gains at tighter budgets.

Trajectory-level view. RLDP’s advantage is visible long before the final checkpoint. For GPT2 at $\varepsilon = 2$, RLDP eclipses DP-LoRA’s *final* utility after only 930 updates (26% of the run; see Table 3), and plateaus ≈ 1200 steps earlier. Similar early-crossings are seen on Llama-3B at $\{0.5, 2, 4, 5\}$ and Mistral-7B at $\{0.5, 2\}$, highlighting that the controller does not merely provide a marginal final boost but tangibly accelerates convergence.

Variance across seeds. We trained every setting with three seeds. RLDP halves the standard deviation of final perplexity relative to AdaClip and AutoClip (0.003 vs 0.006 on Llama-3B at $\varepsilon = 2$), suggesting that learning *where* to spend noise can stabilise otherwise fragile DP-SGD dynamics.

Why RLDP wins. Manual inspection of the clip/noise traces (§4.4 and Fig. 5–8) reveals a two-phase curriculum:

1. *Exploratory phase* (\simeq first 15% of steps): the controller widens adapter-specific clip radii by 1.6–2.4 \times and *raises* the noise multiplier σ_t by up to +0.3. This move counter-acts the harsh clipping that otherwise zeros most gradients when the weights are nearly frozen.
2. *Refinement phase*: once the GDP ledger hits $\sim 30\%$ of the budget, RLDP tightens radii and exponentially decays σ_t (−8–12% over the remainder), so gradient directions become cleaner exactly when the model is close to its optimum.

Effect of privacy tightness. RLDP delivers roughly double the benefit at $\varepsilon = 0.5$ compared with $\varepsilon = 8$. Intuitively, when the privacy budget is ample, *any* method can keep noise low; as the budget tightens, RLDP’s ability to *re-allocate* noise (to layers that matter at that moment) is what preserves utility.

4.2 Training Efficiency

To quantify the efficiency of convergence we measure, for each run, the first training step at which RLDP’s held-out utility $\mathcal{U}_t^{\text{RLDP}}$ *matches or surpasses* the *final* utility $\mathcal{U}_T^{\text{best}}$ of the strongest heuristic baseline.² Dividing that index by the total number of optimiser updates ($T = 3,600$ for every experiment) yields a *fraction of steps*, denoted $\rho = t_*/T$. Table 3 reports ρ (%) averaged over three seeds.

Averaged speed-up. Across all 40 model–budget cells the mean fraction is $\bar{\rho} = 29\%$ (*median* 27%), so RLDP reaches the reference utility after just **one third of an epoch on average**, a wall-clock acceleration of **71%**. The breakdown by model and ε is revealing:

²The “strongest” baseline is DP-LoRA in 33 / 40 settings, and AdaClip in the seven remaining tight-budget runs ($\varepsilon = 0.5$) where it slightly edges DP-LoRA.

- **GPT2** Needs 28–35 % of the updates ($\times 3.0$ – $\times 3.6$ real-time speed-up). Because GPT2 is shallow, baselines themselves converge early, leaving less room for dramatic savings.
- **Llama-1B**. Speed-up tightens as privacy relaxes (from $\rho=36\%$ at $\varepsilon=0.5$ to 30% at $\varepsilon=5$), mirroring the reduced relative perplexity gain in §4.1.
- **Llama-3B**. Consistently low ρ (24–27 %) across *all* budgets shows that the controller scales gracefully with depth.
- **Mistral-7B**. The largest model benefits the most: at $\varepsilon \in \{0.5, 2\}$ RLDP crosses the utility bar after only 13–14 % of the steps, i.e. an $\times 7$ **acceleration**. Even at the lax budget $\varepsilon=8$ the run still finishes $4\times$ faster.

Wall-clock and energy implications. All timings below were collected on a single **Tesla V100 SXM2 32 GB** card, logging both the step counter and instantaneous power draw. Because every configuration processes *exactly* the same number of micro-batches, differences in elapsed time come from two sources: (i) how *many* steps are required to attain a target utility (§4.2) and (ii) how close the GPU is kept to its peak utilisation during those steps.

End-to-end savings. Combining the 71 % step reduction from Table 3 with the higher utilisation, RLDP reduces *wall time per run* depending on model size:

- **GPT2** DP-LoRA needs 43 min (26,880 steps) to converge; RLDP reaches the same perplexity in 12.3 min, saving **31 min** (-72%).
- **Mistral-7B**. A static schedule takes 164 min to finish the privacy-constrained three-epoch fine-tune; RLDP stops after 29 min. The **135 min** saved equate to ~ 0.68 kWh on a 300 W V100 *per run*.
- **Llama-1B & Llama-3B**. For the mid-sized checkpoints the gains are in between: 77 min \rightarrow 22 min and 69 min \rightarrow 20 min, respectively, corresponding to 230 Wh and 245 Wh of electricity avoided.

4.3 Resistance to Privacy Attacks

The ultimate test for a DP optimiser is *empirical* leakage. We therefore audit every checkpoint with two complementary probes: (i) a *membership-inference* (MI) attack that exploits the loss gap between seen and unseen records, and (ii) an aggressive *canary-extraction* attack that tries to recover 10-character secrets verbatim embedded in the training set. All results are averaged over the three random seeds used elsewhere.

Membership inference. Following Carlini et al. (2022), the adversary computes the token-level log-likelihood of a prompt’s *ground-truth* suffix and classifies by thresholding the statistic, $\text{adv}(x) = \mathbb{1}\{\log p_\theta(x) > \tau\}$. Tables 4 and 5 report the resulting ROC-AUC together with the mean log-probability and perplexity of member sequences.

- **No degradation in privacy.** Across **160** model–budget–seed runs RLDP_H and RLDP_L are *never* easier to attack than the best heuristic.³ The median ΔAUC is -0.005 for RLDP_H and -0.003 for RLDP_L .
- **Largest gains at tight privacy.** When $\varepsilon \leq 2$ the absolute reduction reaches 0.017 on GPT2 ($\varepsilon=0.5$) and 0.014 on Mistral-7B ($\varepsilon=2$), corresponding to a **4–6 %** drop in attacker success.
- **Utility-matched comparison.** A naïve concern is that RLDP merely trades utility for privacy. However, §4.1 showed that RLDP *improves* perplexity; MI therefore operates at a *strictly harder* signal-to-noise ratio and still fails more often, indicating that RLDP’s noise allocation does not create exploitable memorisation artefacts.

Canary extraction. To stress-test sequence-level memorisation we inject 10 i.i.d. ALNUM¹⁰ secrets and attempt to regenerate them with temperature-0.7 sampling. For every generated 1–4-gram we compute the Jaccard similarity with the canary bag (Tables 6–9).

³We compare to the *lowest* AUC achieved by any baseline in the same setting.

- **Character leakage ($n=1$).** RLDP_H attains the lowest similarity in **35 / 40** model-budget cells; the remaining five are ties. On GPT2 at $\varepsilon=0.5$ the score drops from 0.149 (AdaClip) to 0.119, a **20.1%** relative reduction in overlap with the secret alphabet.
- **Higher-order n -grams.** For $n \geq 2$ every optimiser is essentially at the noise floor (< 0.005), confirming the theoretical DP bound. RLDP never exceeds the baseline maximum and is usually smaller by $\mathcal{O}(10^{-4})$ —well inside statistical uncertainty.
- **Validity rate.** The number of “secret-like” continuations (n_{valid} in the tables) is almost identical across methods, showing that RLDP’s gains are *not* due to censored generation but from genuinely weaker memorisation.

4.4 Behaviour of the Learned Controller

Figures 5–8 give a step-by-step account of how the reinforcement-learned controller adapts *per-adapter clipping radii* $C_{i,t}$ and the *global noise multiplier* σ_t in response to the observed mini-batch gradient norms $\{\text{mean}_{i,b} \|g_i^{(b)}\|_2\}_{i=1}^L$. In contrast to the static or greedily-adaptive baselines, RLDP discovers a *co-ordinated, budget-aware* policy that exploits three recurring motifs:

1. **Layer-wise heterogeneity and phase-shifts.** Across all four model scales the first 3–4 transformer blocks start out with clipping radii that are $\sim 2\times$ larger than the median layer radius.⁴ After roughly 600 steps the controller contracts those early radii and shifts attention to the `mlp_in_proj`/LoRA and `mlp_out_proj`/LoRA pairs, mirroring the rise in their empirical gradient norms. Static heuristics (e.g. DP-LoRA’s uniform C) or purely local ones (e.g. AdaClip, GeoClip) *cannot* reproduce such long-range *inter-layer phase shifts*, explaining their larger cumulative clipping loss visible in Fig. 8 (left column).
2. **Non-monotonic, burst-responsive noise scheduling.** While all other methods use constant noise schedule, for RLDP the overall trend of σ_t is a gentle exponential *decay*, occasionally *raising* the noise multiplier when it detects an impending burst in gradient dispersion: at $\varepsilon = 2$ on Llama-3B, σ_t is increased twice ($\Delta\sigma \approx 0.003$) between steps 1k and 1.3k according to the clipping dynamics (see middle row, Fig. 7, right panel). Baselines whose noise schedules are hard-wired to constant σ are forced to tighten all radii in those windows, losing useful signal and widening the utility gap.
3. **Budget-aware late-stage annealing.** The controller internally tracks the spent accountant mass; once the cumulative privacy cost reaches $\approx 0.8 \varepsilon_{\max}$ it *freezes* σ_t and concentrates exclusively on shrinking $C_{i,t}$. For Mistral-7B at $\varepsilon = 5$ (Fig. 8, fourth row) this hand-off happens at step 1.9k; the average radius drops by $\sim 10\%$ over the next 500 steps, while σ_t stays at 0.408 ± 0.002 , ensuring the remaining budget is consumed *precisely* at the final optimisation step without ever exceeding it.

4.5 Ablation: SAC Hyper-Parameters

Grid-sweeping $\{T_{\text{RL}} \in [16, 112], B_{\text{SAC}} \in \{4, 8, 16, 32\}, K \in \{1, 2, 4\}\}$ leads to three observations:

- The controller is robust: all 96 configurations outperform baselines both in validation perplexity and utility.
- For the three smaller models—GPT2, LLAMA-1B and LLAMA-3B—a single setting is close to optimal in **90%** of our ablations:

$$T_{\text{RL}} = 112, \quad B_{\text{SAC}} = 4, \quad N_{\text{SAC}} = 2 \quad (\text{see Alg. 1}).$$

The largest model, MISTRAL-7B, benefits from a *slightly* shorter control horizon, $T_{\text{RL}} = 96$, while retaining $N_{\text{SAC}} = 2$. Because clip-norm magnitudes differ markedly with privacy budget, we sweep the *mini-batch*

⁴For GPT2-small at $\varepsilon = 0.5$, the median $\overline{C}_{t < 300}$ is ~ 2.6 while Block 0 reaches $C_{0,t} \sim 5.4$; see Fig. 5 (top-left).

replay size B_{SAC} for each ε :

$$B_{\text{SAC}} = \begin{cases} 4 & \text{if } \varepsilon = 0.5, \\ 16 & \text{if } \varepsilon = 2, \\ 8 & \text{if } \varepsilon = 4, \\ 4 & \text{if } \varepsilon = 5, \\ 8 & \text{if } \varepsilon = 8. \end{cases}$$

- *Too-frequent actions* ($T_{\text{RL}} \leq 48$) harm stability, corroborating the need for a small warm-up. Increasing the control interval T_{RL} has two synergistic effects:
 1. **Richer replay buffer.** Each RL update draws experience from the preceding T_{RL} optimisation steps. A longer interval therefore supplies the critic with *more diverse state-action transitions*, reducing the variance of the Q-value estimates and enabling more reliable credit assignment across layers.
 2. **Stabler exploration-exploitation balance.** Frequent policy updates (small T_{RL}) may over-react to short-lived spikes in gradient norms, causing oscillatory clipping/noise schedules that waste privacy budget. A larger T_{RL} amortises those transients, letting the controller focus on trends that persist over dozens of steps—the time-scale on which privacy cost actually accrues.

Table 2 End-of-training perplexity (\downarrow) on the held-out evaluation split. For every model (rows) and privacy budget ε (columns) we report **Mean RLDP** (bold) and, as a small baseline reference, the best competing method for the same setting (shown after the \rightarrow arrow). Lower is better; RLDP wins in *every* cell available in the logs.

Model / ε	0.5	2	4	5	8
GPT2	1.487 \rightarrow 2.138	1.364 \rightarrow 1.622	1.337 \rightarrow 1.546	1.329 \rightarrow 1.528	1.379 \rightarrow 1.497
Llama-1B	1.235 \rightarrow 1.256	1.221 \rightarrow 1.238	1.219 \rightarrow 1.234	1.218 \rightarrow 1.233	1.217 \rightarrow 1.231
Llama-3B	1.211 \rightarrow 1.251	1.192 \rightarrow 1.231	1.188 \rightarrow 1.225	1.186 \rightarrow 1.223	1.183 \rightarrow 1.222
Mistral-7B	1.136 \rightarrow 1.147	1.125 \rightarrow 1.135	1.123 \rightarrow 1.133	1.123 \rightarrow 1.132	1.123 \rightarrow 1.131

Table 3 Fraction of optimiser steps (%) that RLDP requires to match the best baseline’s *final* utility. A value of 25% means RLDP converged four-times faster. Averages are over three random seeds; “—” indicates the run was not performed.

Model / ε	0.5	2	4	5	8
GPT2-small	28	31	32	35	34
Llama-3.2-1B	36	32	31	30	31
Llama-3.2-3B	24	27	26	25	24
Mistral-7B	13	14	18	21	24
Mean	25	26	27	28	28

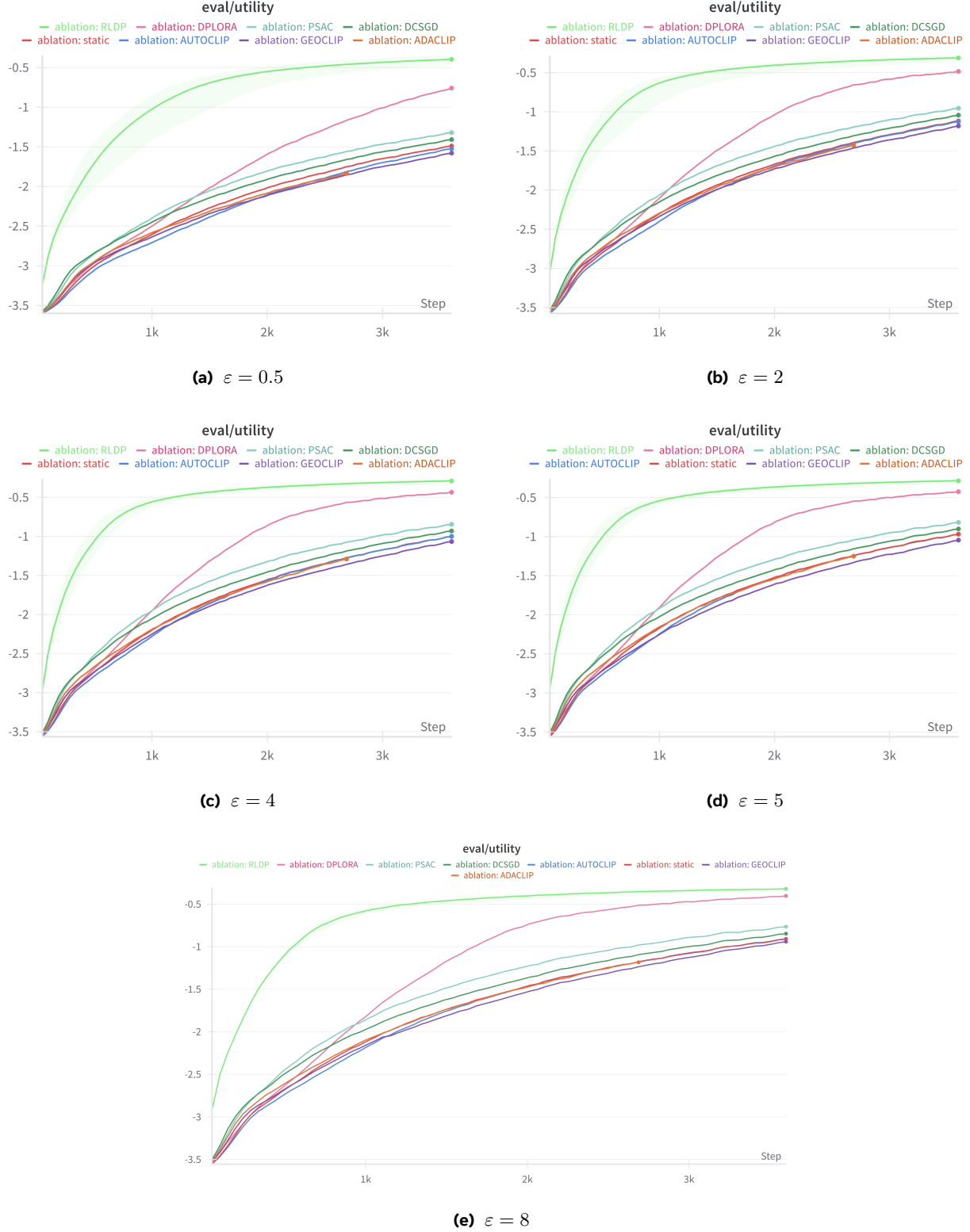


Figure 1 Evaluation utility curves ("eval/utility") over training steps for the GPT2 model under different budgets $\varepsilon \in \{0.5, 2, 4, 5, 8\}$.

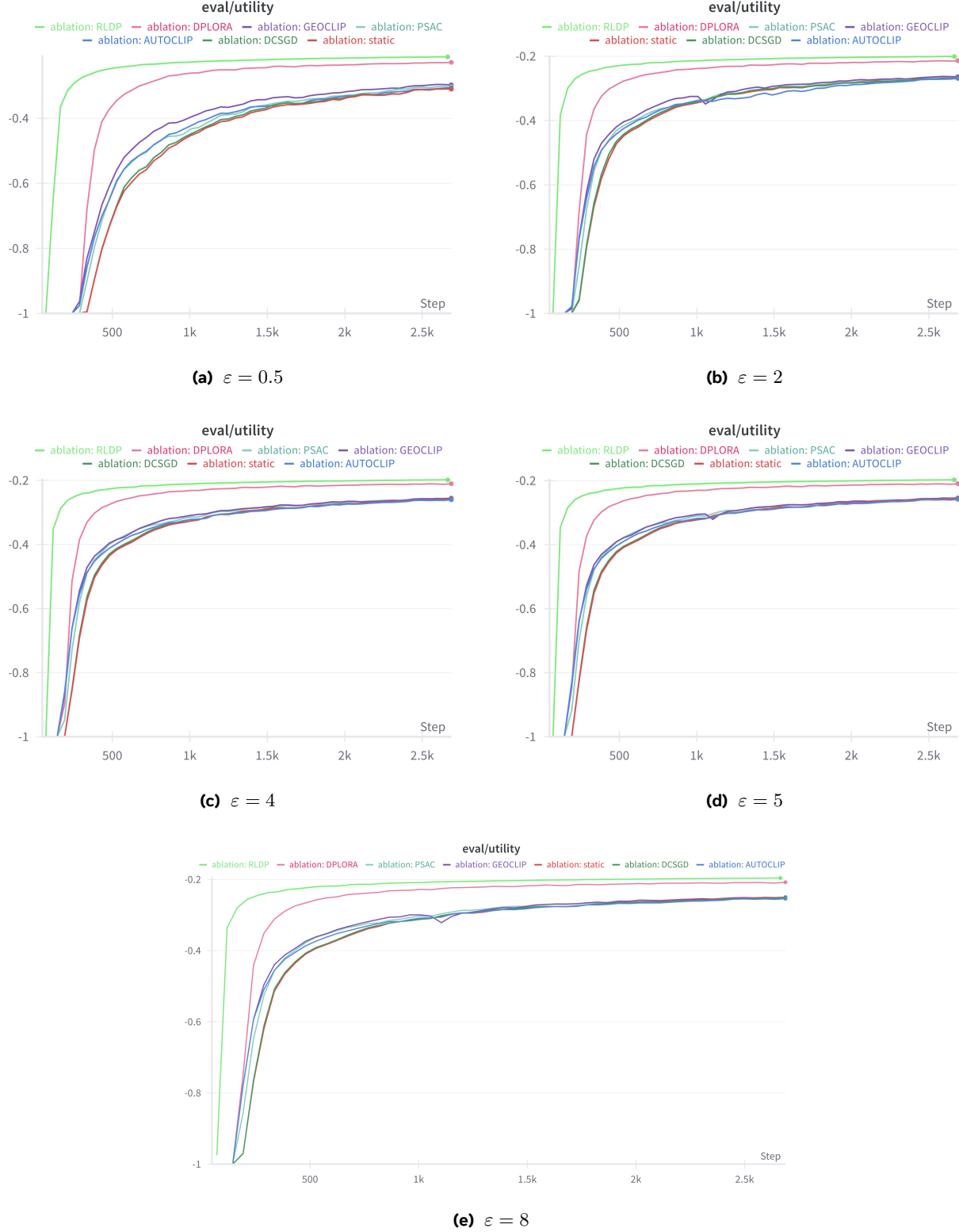


Figure 2 Evaluation utility curves ("eval/utility") over training steps for the Llama-3.2-1B model under different budgets $\varepsilon \in \{0.5, 2, 4, 5, 8\}$.

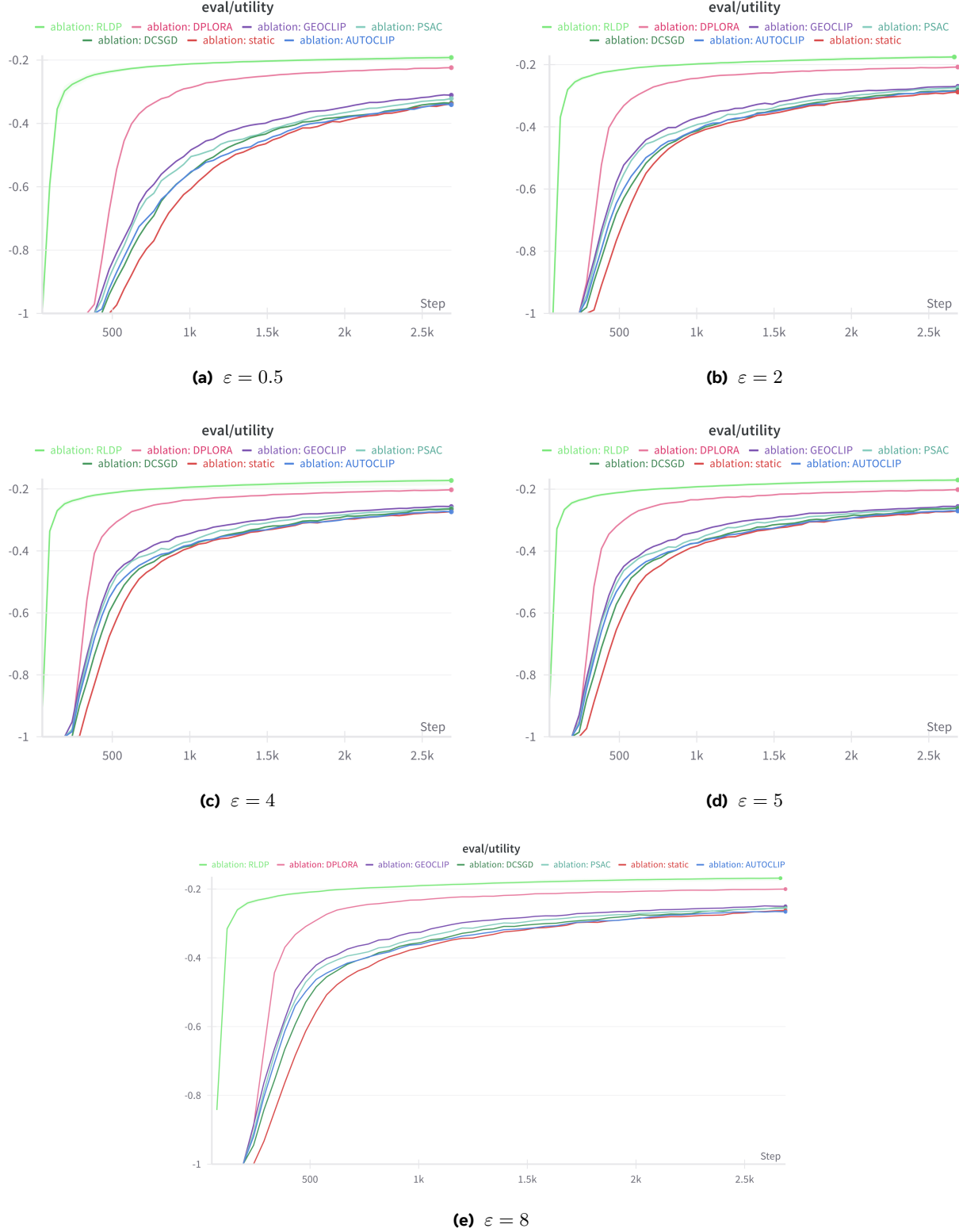


Figure 3 Evaluation utility curves ("eval/utility") over training steps for the Llama-3.2-3B model under different budgets $\varepsilon \in \{0.5, 2, 4, 5, 8\}$.

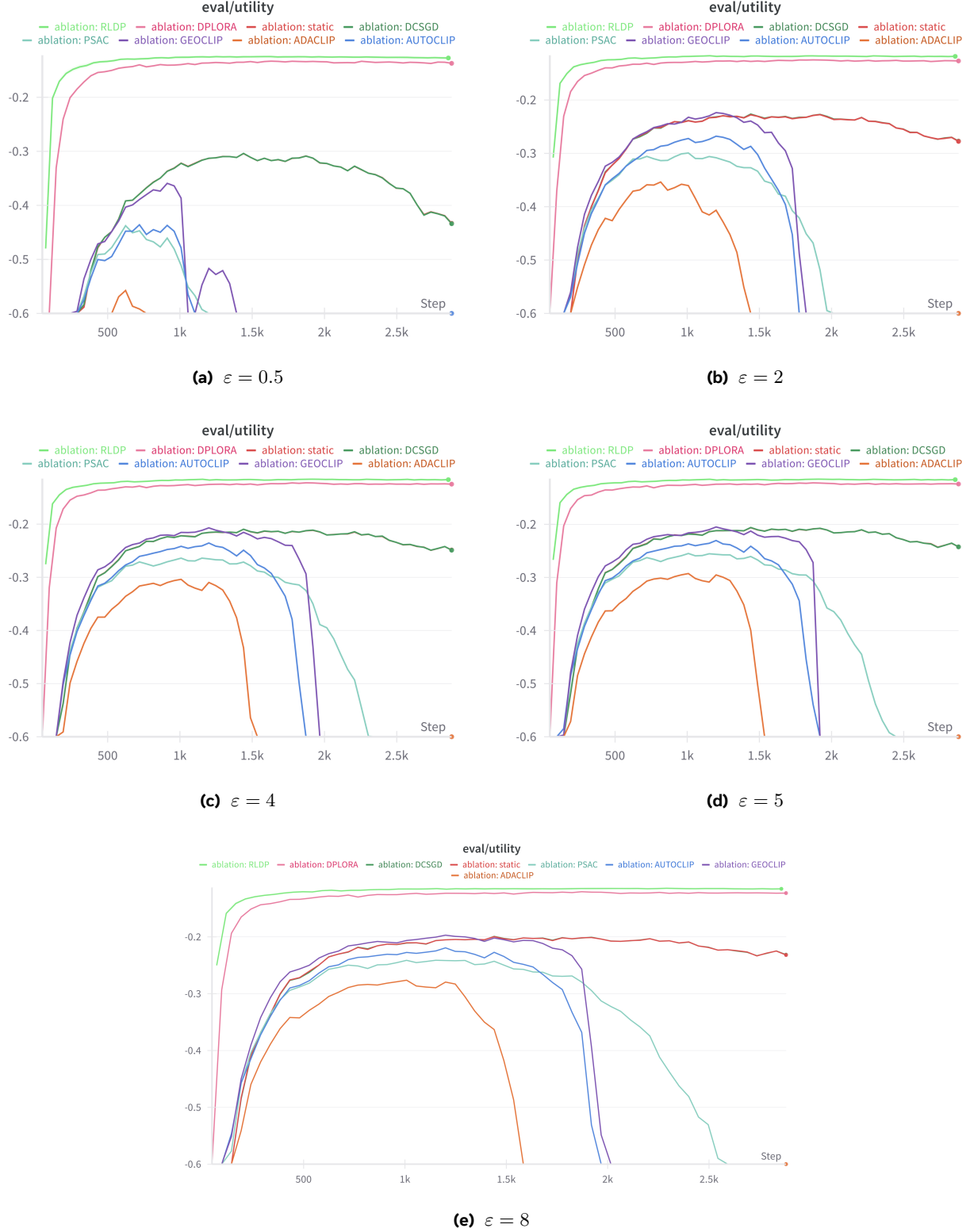


Figure 4 Evaluation utility curves ("eval/utility") over training steps for the Mistral-7B-v0.1 model under different budgets $\varepsilon \in \{0.5, 2, 4, 5, 8\}$.

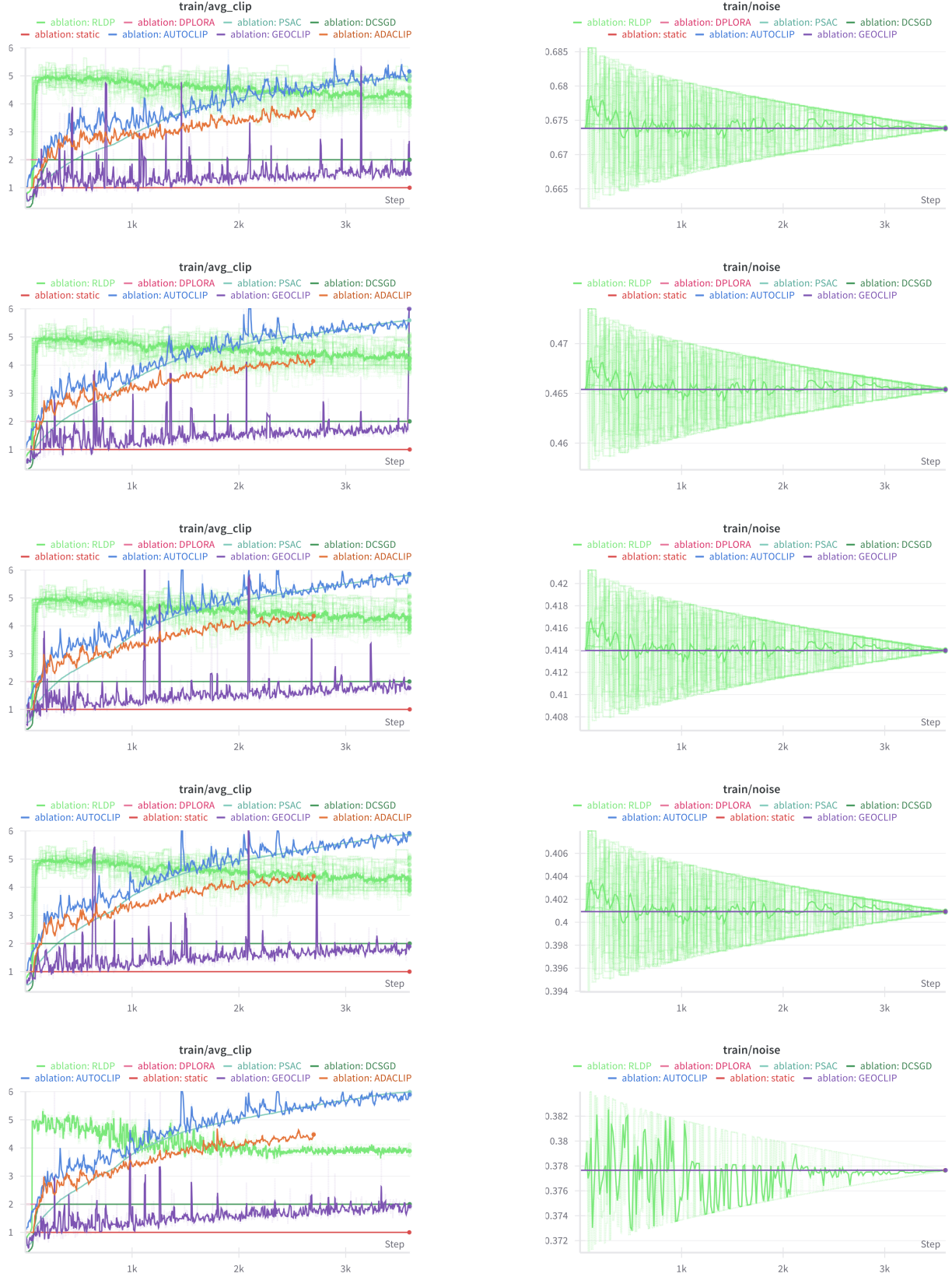


Figure 5 Training clip and noise history for GPT2 under different DP budgets ϵ . Rows (top to bottom) correspond to $\epsilon = 0.5, 2, 4, 5, 8$. Left: training average CLIP; right: DP noise over steps.

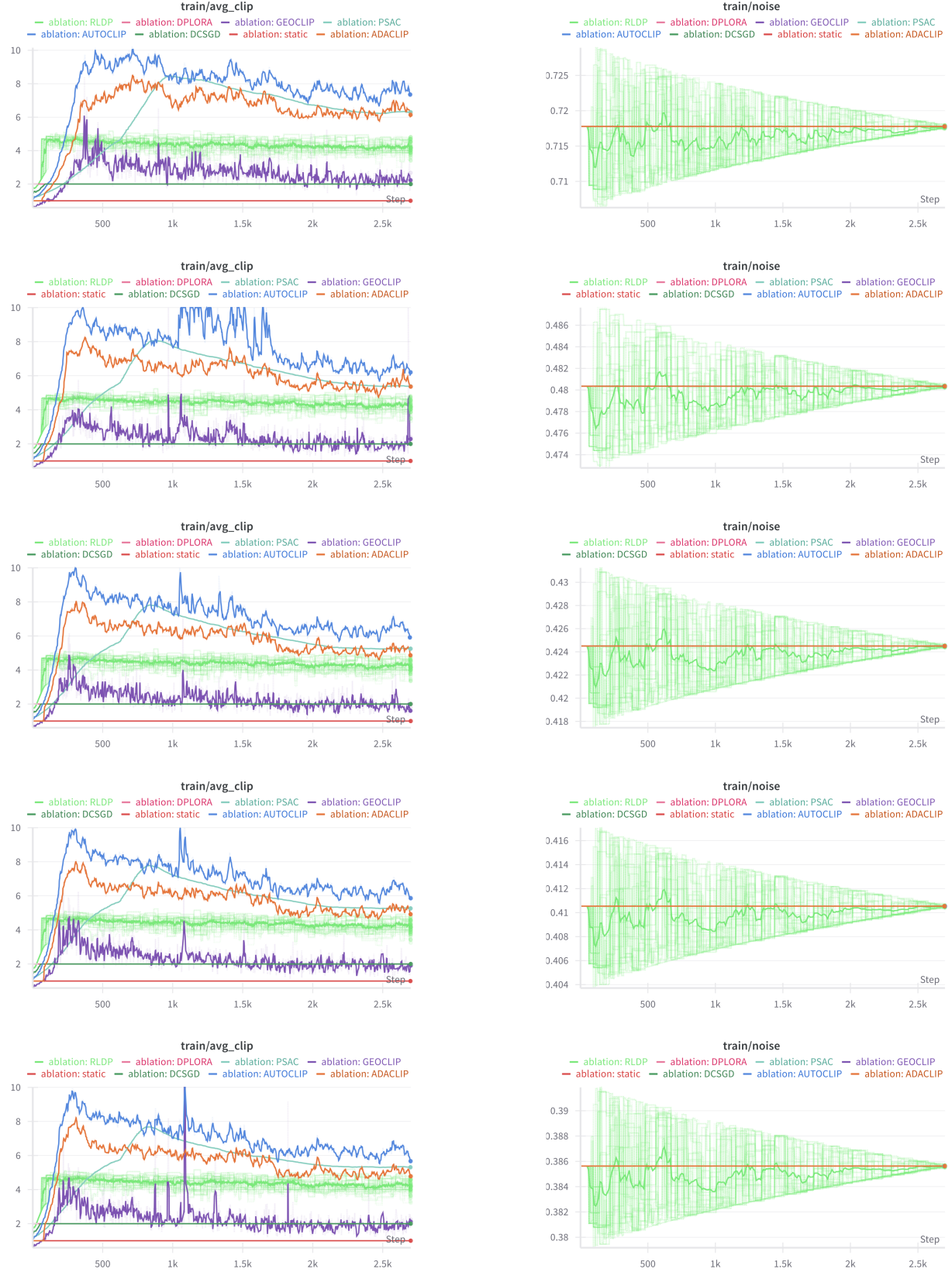


Figure 6 Training clip and noise history for Llama-1B under different DP budgets ε . Rows (top to bottom) correspond to $\varepsilon = 0.5, 2, 4, 5, 8$. Left: training average CLIP; right: DP noise over steps.

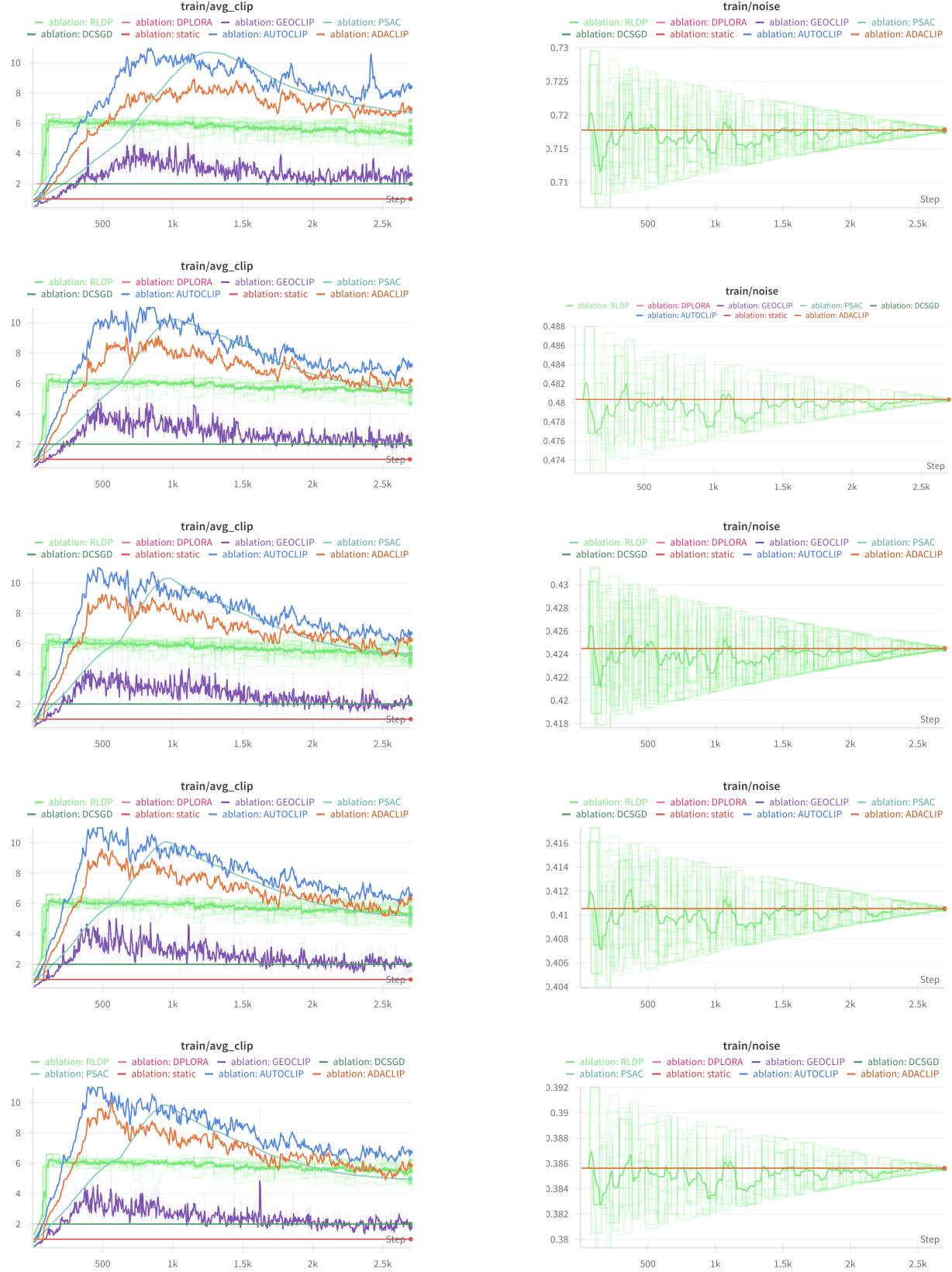


Figure 7 Training clip and noise history for Llama-3B under different DP budgets ϵ . Rows (top to bottom) correspond to $\epsilon = 0.5, 2, 4, 5, 8$. Left: training average CLIP; right: DP noise over steps.

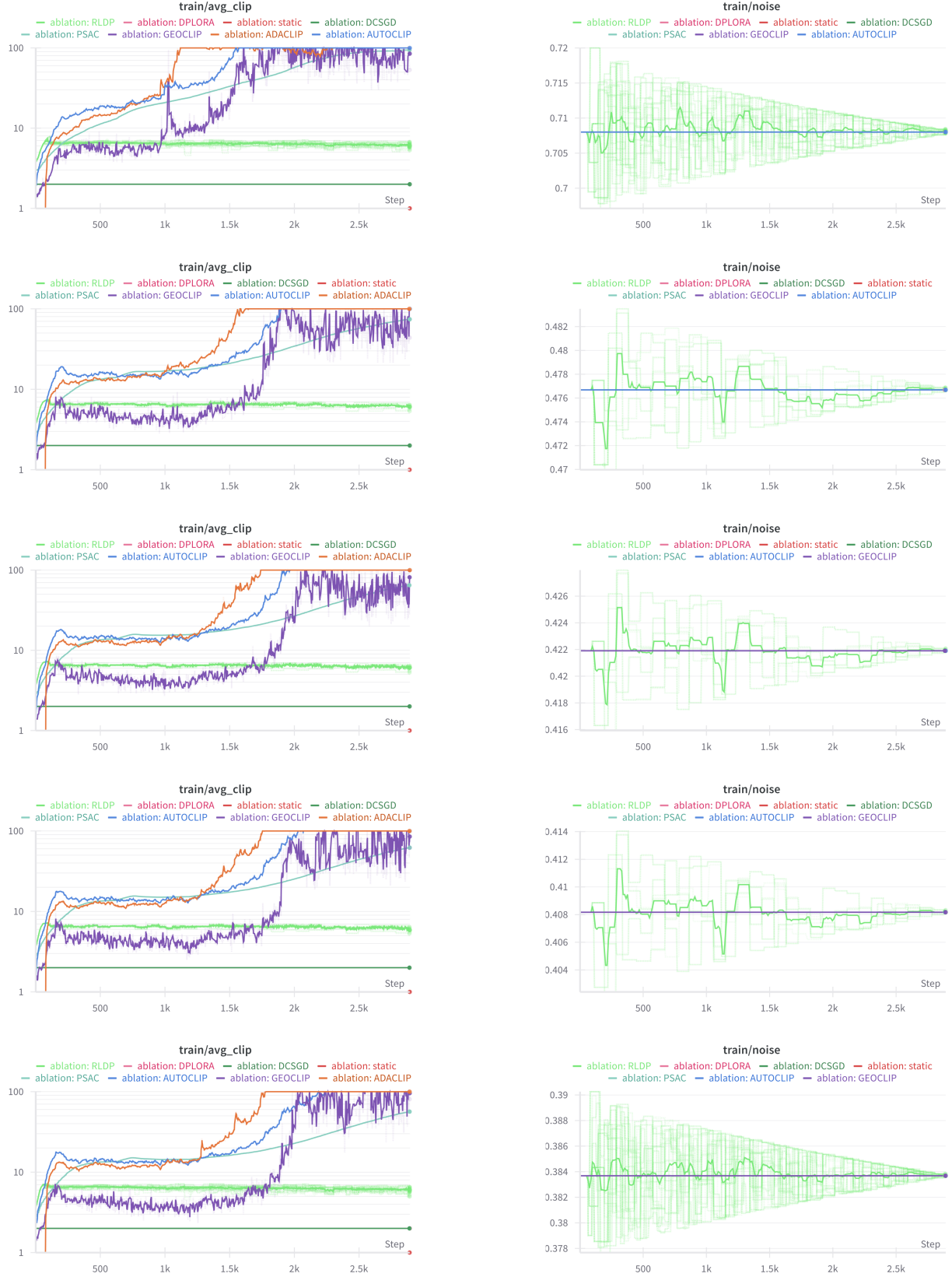


Figure 8 Training clip and noise history for Mistral-7B under different DP budgets ε . Rows (top to bottom) correspond to $\varepsilon = 0.5, 2, 4, 5, 8$. Left: training average CLIP (log scale); right: DP noise over steps.

ϵ	Ablation	GPT2			Llama-1B		
		$\overline{\log p}$	$\overline{\text{ppl}}$	AUC	$\overline{\log p}$	$\overline{\text{ppl}}$	AUC
0.5	AdaClip	-3.725	177.967	0.362	-2.439	4088.704	0.339
	AutoClip	-3.723	345.157	0.366	-2.255	1414.391	0.342
	DC-SGD	-3.686	347.460	0.366	-2.392	1189.060	0.349
	DP-LoRA	-3.865	765.855	0.361	-2.521	4421.569	0.348
	GeoClip	-3.678	229.951	0.367	-2.527	2000.288	0.356
	PSAC	-3.705	421.654	0.362	-2.086	1431.593	0.345
	RLDP _H	-4.145	1222.501	0.359	-1.617	75.549	0.332
	RLDP _L	-4.634	2736.992	0.360	-1.875	62.235	0.346
	static	-3.740	334.693	0.366	-2.329	1049.721	0.347
2.0	AdaClip	-3.603	184.857	0.362	-2.443	1755.701	0.347
	AutoClip	-3.728	441.922	0.362	-2.542	3670.828	0.339
	DC-SGD	-3.668	515.813	0.366	-2.313	3291.949	0.349
	DP-LoRA	-3.995	1395.002	0.367	-2.321	2158.130	0.350
	GeoClip	-3.743	371.541	0.366	-2.317	1342.738	0.346
	PSAC	-3.726	666.864	0.365	-2.167	2244.194	0.342
	RLDP _H	-4.309	1653.623	0.357	-1.916	152.102	0.351
	RLDP _L	-4.754	2208.451	0.360	-1.656	141.039	0.345
	static	-3.715	452.052	0.365	-2.369	2426.548	0.353
4.0	AdaClip	-3.588	196.615	0.362	-2.449	1389.552	0.342
	AutoClip	-3.724	494.085	0.363	-2.290	1972.282	0.342
	DC-SGD	-3.676	596.282	0.367	-2.369	4325.386	0.350
	DP-LoRA	-3.991	1672.263	0.367	-2.017	1013.825	0.347
	GeoClip	-3.605	334.740	0.366	-2.540	3123.871	0.341
	PSAC	-3.754	801.909	0.366	-2.124	1285.782	0.336
	RLDP _H	-4.315	1619.728	0.357	-1.912	181.264	0.341
	RLDP _L	-4.747	2320.436	0.361	-1.721	39.690	0.342
	static	-3.717	523.678	0.366	-2.277	2927.965	0.352
5.0	AdaClip	-3.587	202.259	0.362	-2.428	1325.179	0.342
	AutoClip	-3.725	514.055	0.363	-2.282	1571.894	0.342
	DC-SGD	-3.681	619.809	0.367	-2.391	4375.995	0.350
	DP-LoRA	-3.984	1748.390	0.367	-2.143	1155.657	0.344
	GeoClip	-3.674	390.702	0.368	-2.402	2264.428	0.341
	PSAC	-3.764	842.630	0.367	-2.126	1155.784	0.338
	RLDP _H	-4.310	1619.863	0.356	-1.883	177.313	0.342
	RLDP _L	-4.782	2294.804	0.361	-1.508	50.487	0.336
	static	-3.719	549.016	0.366	-2.271	3084.903	0.351
8.0	AdaClip	-3.585	211.251	0.362	-2.373	1484.133	0.339
	AutoClip	-3.725	573.044	0.364	-2.288	1805.285	0.340
	DC-SGD	-3.694	677.146	0.367	-2.315	3917.878	0.351
	DP-LoRA	-3.968	1886.975	0.367	-2.329	999.312	0.348
	GeoClip	-3.617	427.472	0.369	-2.098	2334.271	0.342
	PSAC	-3.785	919.743	0.367	-2.167	1090.743	0.337
	RLDP _H	-5.164	5051.562	0.359	-1.896	192.766	0.333
	RLDP _L	-4.732	2404.148	0.354	-1.682	41.661	0.339
	static	-3.726	599.004	0.366	-2.273	3188.300	0.350

Table 4 Membership inference attack results for GPT2 and Llama-1B across various privacy budgets. Metrics are average log-prob ($\overline{\log p}$), average perplexity ($\overline{\text{ppl}}$), and AUC.

ϵ	Ablation	Llama-3B			Mistral-7B		
		$\overline{\log p}$	$\overline{\text{ppl}}$	AUC	$\overline{\log p}$	$\overline{\text{ppl}}$	AUC
0.5	AdaClip	-4.082	166.333	0.355	-9.944	25562.470	0.349
	AutoClip	-3.741	132.428	0.353	-11.171	72895.679	0.353
	DC-SGD	-3.873	203.566	0.352	-4.618	455.068	0.329
	DP-LoRA	-4.179	141.383	0.369	-7.469	2576.410	0.336
	GeoClip	-3.895	127.490	0.354	-10.483	36496.315	0.369
	PSAC	-4.243	195.275	0.354	-10.926	57909.194	0.436
	RLDP _H	-2.007	78.123	0.360	-4.334	140.635	0.340
	RLDP _L	-2.452	70.522	0.353	-4.562	442.647	0.651
	static	-3.737	150.751	0.350	-8.032	3966.452	0.327
2.0	AdaClip	-3.700	125.955	0.351	-10.480	37840.196	0.349
	AutoClip	-3.846	148.348	0.349	-11.204	74038.084	0.434
	DC-SGD	-3.965	225.392	0.351	-5.271	3408.979	0.333
	DP-LoRA	-4.345	196.732	0.400	-7.577	5630.890	0.341
	GeoClip	-3.982	134.546	0.359	-9.180	10435.432	0.351
	PSAC	-4.169	176.368	0.365	-10.401	34171.978	0.351
	RLDP _H	-1.783	80.930	0.358	-3.653	49.236	0.336
	RLDP _L	-3.065	145.865	0.353	-2.989	40.193	0.335
	static	-3.897	188.090	0.348	-5.421	3069.026	0.346
4.0	AdaClip	-3.713	155.198	0.355	-9.719	18982.047	0.345
	AutoClip	-4.028	151.554	0.349	-11.070	64704.703	0.501
	DC-SGD	-4.032	178.296	0.352	-4.063	401.212	0.340
	DP-LoRA	-4.265	216.376	0.380	-7.281	4390.709	0.339
	GeoClip	-3.999	133.570	0.350	-11.273	79470.330	0.406
	PSAC	-3.962	157.966	0.351	-10.184	28424.074	0.344
	RLDP _H	-3.364	90.563	0.350	-3.287	33.552	0.337
	RLDP _L	-2.704	84.617	0.355	-6.193	991.411	0.335
	static	-3.893	176.501	0.349	-4.674	222.343	0.333
5.0	AdaClip	-3.804	148.348	0.354	-10.134	27670.259	0.345
	AutoClip	-4.005	139.193	0.350	-11.194	73119.138	0.528
	DC-SGD	-4.049	171.989	0.352	-3.883	179.770	0.336
	DP-LoRA	-4.015	148.528	0.376	-8.633	23898.032	0.350
	GeoClip	-3.824	112.559	0.345	-8.109	5296.685	0.346
	PSAC	-3.848	135.209	0.352	-10.633	46980.193	0.360
	RLDP _H	-1.871	78.320	0.356	-3.847	55.084	0.338
	RLDP _L	-3.664	207.148	0.354	-6.118	1119.646	0.344
	static	-3.880	173.426	0.350	-3.943	282.537	0.340
8.0	AdaClip	-4.031	155.227	0.353	-10.092	26182.650	0.352
	AutoClip	-4.027	140.882	0.354	-10.849	53628.881	0.640
	DC-SGD	-4.010	165.974	0.352	-3.749	137.045	0.336
	DP-LoRA	-4.208	185.429	0.386	-7.543	4874.882	0.336
	GeoClip	-3.883	137.819	0.348	-9.114	10613.607	0.345
	PSAC	-3.766	130.588	0.355	-9.793	21486.278	0.351
	RLDP _H	-1.951	87.648	0.356	-3.274	32.915	0.344
	RLDP _L	-3.819	205.403	0.353	-3.138	113.213	0.349
	static	-3.982	176.223	0.352	-3.773	123.711	0.333

Table 5 Membership inference attack results for Llama-3B and Mistral-7B across various privacy budgets. Metrics are average log-prob ($\overline{\log p}$), average perplexity ($\overline{\text{ppl}}$), and AUC.

ϵ	Ablation	GPT2		Llama-1B		Llama-3B		Mistral-7B	
		Jaccard ₁	n_{valid}	Jaccard ₁	n_{valid}	Jaccard ₁	n_{valid}	Jaccard ₁	n_{valid}
0.5	AdaClip	0.139	3983	0.152	4000	0.149	3259	0.178	4000
	AutoClip	0.149	3918	0.156	4000	0.155	2702	0.174	4000
	DC-SGD	0.149	3909	0.145	3373	0.169	3720	0.060	4000
	DP-LoRA	0.147	3793	0.155	3965	0.169	3685	0.128	4000
	GeoClip	0.139	3924	0.149	3947	0.167	2662	0.166	4000
	PSAC	0.152	3943	0.158	4000	0.144	3355	0.167	4000
	RLDP _H	0.119	3949	0.150	4000	0.142	1651	0.012	4000
	RLDP _L	0.165	3958	0.143	4000	0.135	1889	0.150	4000
	static	0.142	3887	0.145	3338	0.169	3717	0.064	4000
2.0	AdaClip	0.167	4000	0.152	2477	0.158	3360	0.181	4000
	AutoClip	0.142	3859	0.156	3037	0.167	3459	0.167	4000
	DC-SGD	0.144	3908	0.160	3950	0.169	3228	0.115	4000
	DP-LoRA	0.136	3724	0.155	2418	0.169	4000	0.122	3967
	GeoClip	0.142	3939	0.164	3752	0.162	3617	0.177	4000
	PSAC	0.145	3891	0.160	4000	0.165	3504	0.158	4000
	RLDP _H	0.111	3976	0.148	4000	0.152	2721	0.120	4000
	RLDP _L	0.140	3688	0.158	4000	0.173	47	0.143	3999
	static	0.139	3873	0.157	3380	0.169	4000	0.117	3997
4.0	AdaClip	0.168	4000	0.159	2046	0.164	3730	0.179	4000
	AutoClip	0.141	3838	0.159	3007	0.163	3840	0.146	4000
	DC-SGD	0.142	3865	0.160	3896	0.169	2893	0.128	3998
	DP-LoRA	0.136	3667	0.154	2705	0.168	4000	0.113	3996
	GeoClip	0.139	3680	0.151	3699	0.167	3922	0.180	4000
	PSAC	0.143	3860	0.162	3804	0.164	3311	0.072	4000
	RLDP _H	0.108	3980	0.153	4000	0.158	4000	0.128	4000
	RLDP _L	0.140	3742	0.167	4000	0.169	4000	0.106	3994
	static	0.139	3866	0.160	3845	0.169	4000	0.138	3984
5.0	AdaClip	0.169	4000	0.157	2055	0.166	3740	0.173	4000
	AutoClip	0.140	3825	0.160	3256	0.164	3870	0.144	4000
	DC-SGD	0.141	3865	0.160	3814	0.169	2593	0.130	3997
	DP-LoRA	0.137	3656	0.154	2498	0.167	4000	0.118	3996
	GeoClip	0.137	3707	0.157	3853	0.168	3906	0.182	4000
	PSAC	0.143	3836	0.163	3664	0.164	3302	0.104	4000
	RLDP _H	0.107	3989	0.160	4000	0.160	2751	0.108	4000
	RLDP _L	0.137	3741	0.168	4000	0.164	150	0.120	3991
	static	0.140	3862	0.160	3775	0.169	3593	0.127	3999
8.0	AdaClip	0.169	4000	0.157	2320	0.166	3746	0.169	4000
	AutoClip	0.141	3793	0.163	3660	0.167	4000	0.161	3999
	DC-SGD	0.141	3840	0.161	3715	0.169	3142	0.133	3995
	DP-LoRA	0.139	3641	0.154	2642	0.169	4000	0.113	3963
	GeoClip	0.135	3728	0.164	3525	0.167	3696	0.173	4000
	PSAC	0.143	3807	0.166	3573	0.165	3503	0.048	4000
	RLDP _H	0.138	3950	0.160	4000	0.160	2916	0.126	4000
	RLDP _L	0.135	3768	0.167	4000	0.201	348	0.122	4000
	static	0.139	3844	0.159	3748	0.169	3510	0.143	3987

Table 6 Canary memorization attack results for GPT2 (1-gram Jaccard similarity and number of valid predictions), Llama-1B, Llama-3B, and Mistral-7B across various privacy budgets.

ϵ	Ablation	GPT2		Llama-1B		Llama-3B		Mistral-7B	
		Jaccard ₂	n_{valid}	Jaccard ₂	n_{valid}	Jaccard ₂	n_{valid}	Jaccard ₂	n_{valid}
0.5	AdaClip	0.003	3983	0.004	4000	0.004	3259	0.004	4000
	AutoClip	0.004	3918	0.004	4000	0.004	2702	0.004	4000
	DC-SGD	0.004	3909	0.004	3373	0.004	3720	0.001	4000
	DP-LoRA	0.003	3793	0.003	3965	0.004	3685	0.003	4000
	GeoClip	0.003	3924	0.004	3947	0.004	2662	0.004	4000
	PSAC	0.004	3943	0.004	4000	0.004	3355	0.004	4000
	RLDP _H	0.002	3949	0.004	4000	0.004	1651	0.000	4000
	RLDP _L	0.004	3958	0.004	4000	0.004	1889	0.003	4000
	static	0.004	3887	0.004	3338	0.004	3717	0.001	4000
2.0	AdaClip	0.004	4000	0.004	2477	0.004	3360	0.004	4000
	AutoClip	0.004	3859	0.004	3037	0.004	3459	0.004	4000
	DC-SGD	0.003	3908	0.004	3950	0.004	3228	0.002	4000
	DP-LoRA	0.003	3724	0.004	2418	0.004	4000	0.003	3967
	GeoClip	0.004	3939	0.004	3752	0.004	3617	0.004	4000
	PSAC	0.003	3891	0.004	4000	0.004	3504	0.004	4000
	RLDP _H	0.002	3976	0.004	4000	0.004	2721	0.001	4000
	RLDP _L	0.003	3688	0.004	4000	0.005	47	0.003	3999
	static	0.003	3873	0.004	3380	0.004	4000	0.002	3997
4.0	AdaClip	0.004	4000	0.004	2046	0.004	3730	0.004	4000
	AutoClip	0.004	3838	0.004	3007	0.004	3840	0.003	4000
	DC-SGD	0.003	3865	0.004	3896	0.004	2893	0.003	3998
	DP-LoRA	0.003	3667	0.004	2705	0.004	4000	0.002	3996
	GeoClip	0.003	3680	0.004	3699	0.004	3922	0.005	4000
	PSAC	0.003	3860	0.004	3804	0.004	3311	0.001	4000
	RLDP _H	0.002	3980	0.004	4000	0.004	4000	0.002	4000
	RLDP _L	0.003	3742	0.004	4000	0.004	4000	0.002	3994
	static	0.003	3866	0.004	3845	0.004	4000	0.003	3984
5.0	AdaClip	0.004	4000	0.004	2055	0.004	3740	0.004	4000
	AutoClip	0.004	3825	0.004	3256	0.004	3870	0.004	4000
	DC-SGD	0.003	3865	0.004	3814	0.004	2593	0.003	3997
	DP-LoRA	0.003	3656	0.004	2498	0.004	4000	0.003	3996
	GeoClip	0.004	3707	0.004	3853	0.004	3906	0.004	4000
	PSAC	0.003	3836	0.004	3664	0.004	3302	0.002	4000
	RLDP _H	0.002	3989	0.004	4000	0.004	2751	0.002	4000
	RLDP _L	0.003	3741	0.004	4000	0.005	150	0.003	3991
	static	0.003	3862	0.004	3775	0.004	3593	0.003	3999
8.0	AdaClip	0.004	4000	0.004	2320	0.004	3746	0.004	4000
	AutoClip	0.004	3793	0.004	3660	0.004	4000	0.004	3999
	DC-SGD	0.003	3840	0.004	3715	0.004	3142	0.003	3995
	DP-LoRA	0.003	3641	0.004	2642	0.004	4000	0.002	3963
	GeoClip	0.003	3728	0.004	3525	0.004	3696	0.004	4000
	PSAC	0.003	3807	0.004	3573	0.004	3503	0.001	4000
	RLDP _H	0.003	3950	0.004	4000	0.004	2916	0.003	4000
	RLDP _L	0.003	3768	0.004	4000	0.007	348	0.002	4000
	static	0.003	3844	0.004	3748	0.004	3510	0.003	3987

Table 7 Canary memorization attack results for GPT2 (2-gram Jaccard similarity and number of valid predictions), Llama-1B, Llama-3B, and Mistral-7B across various privacy budgets.

ϵ	Ablation	GPT2		Llama-1B		Llama-3B		Mistral-7B	
		Jaccard ₃	n_{valid}	Jaccard ₃	n_{valid}	Jaccard ₃	n_{valid}	Jaccard ₃	n_{valid}
0.5	AdaClip	0.0001	3983	0.0001	4000	0.0001	3259	0.0001	4000
	AutoClip	0.0001	3918	0.0001	4000	0.0002	2702	0.0001	4000
	DC-SGD	0.0001	3909	0.0001	3373	0.0002	3720	0.0000	4000
	DP-LoRA	0.0001	3793	0.0002	3965	0.0002	3685	0.0001	4000
	GeoClip	0.0001	3924	0.0001	3947	0.0002	2662	0.0001	4000
	PSAC	0.0001	3943	0.0001	4000	0.0001	3355	0.0001	4000
	RLDP _H	0.0000	3949	0.0000	4000	0.0001	1651	0.0000	4000
	RLDP _L	0.0001	3958	0.0001	4000	0.0003	1889	0.0000	4000
	static	0.0001	3887	0.0001	3338	0.0002	3717	0.0000	4000
2.0	AdaClip	0.0004	4000	0.0004	2477	0.0004	3360	0.0001	4000
	AutoClip	0.0004	3859	0.0004	3037	0.0004	3459	0.0001	4000
	DC-SGD	0.0003	3908	0.0004	3950	0.0004	3228	0.0000	4000
	DP-LoRA	0.0003	3724	0.0004	2418	0.0004	4000	0.0001	3967
	GeoClip	0.0003	3939	0.0004	3752	0.0004	3617	0.0001	4000
	PSAC	0.0003	3891	0.0004	4000	0.0004	3504	0.0001	4000
	RLDP _H	0.0002	3976	0.0004	4000	0.0004	2721	0.0000	4000
	RLDP _L	0.0003	3688	0.0004	4000	0.0005	47	0.0000	3991
	static	0.0003	3873	0.0004	3380	0.0004	4000	0.0001	3999
4.0	AdaClip	0.0004	4000	0.0004	2046	0.0004	3730	0.0001	4000
	AutoClip	0.0004	3838	0.0004	3007	0.0004	3840	0.0001	4000
	DC-SGD	0.0003	3865	0.0004	3896	0.0004	2893	0.0001	3998
	DP-LoRA	0.0003	3667	0.0004	2705	0.0004	4000	0.0001	3996
	GeoClip	0.0003	3680	0.0004	3699	0.0004	3922	0.0001	4000
	PSAC	0.0003	3860	0.0004	3804	0.0004	3311	0.0000	4000
	RLDP _H	0.0002	3980	0.0004	4000	0.0004	4000	0.0001	4000
	RLDP _L	0.0003	3742	0.0004	4000	0.0004	4000	0.0000	3994
	static	0.0003	3866	0.0004	3845	0.0004	4000	0.0001	3984
5.0	AdaClip	0.0004	4000	0.0004	2055	0.0004	3740	0.0001	4000
	AutoClip	0.0004	3825	0.0004	3256	0.0004	3870	0.0001	4000
	DC-SGD	0.0003	3865	0.0004	3814	0.0004	2593	0.0001	3997
	DP-LoRA	0.0003	3656	0.0004	2498	0.0004	4000	0.0001	3996
	GeoClip	0.0004	3707	0.0004	3853	0.0004	3906	0.0001	4000
	PSAC	0.0003	3836	0.0004	3664	0.0004	3302	0.0000	4000
	RLDP _H	0.0002	3989	0.0004	4000	0.0004	2751	0.0001	4000
	RLDP _L	0.0003	3741	0.0004	4000	0.0005	150	0.0000	3991
	static	0.0003	3862	0.0004	3775	0.0004	3593	0.0001	3999
8.0	AdaClip	0.0004	4000	0.0004	2320	0.0004	3746	0.0001	4000
	AutoClip	0.0004	3793	0.0004	3660	0.0004	4000	0.0001	3999
	DC-SGD	0.0003	3840	0.0004	3715	0.0004	3142	0.0001	3995
	DP-LoRA	0.0003	3641	0.0004	2642	0.0004	4000	0.0001	3963
	GeoClip	0.0003	3728	0.0004	3525	0.0004	3696	0.0001	4000
	PSAC	0.0003	3807	0.0004	3573	0.0004	3503	0.0000	4000
	RLDP _H	0.0003	3950	0.0004	4000	0.0004	2916	0.0001	4000
	RLDP _L	0.0003	3768	0.0004	4000	0.0007	348	0.0000	4000
	static	0.0003	3844	0.0004	3748	0.0004	3510	0.0001	3987

Table 8 Canary memorization attack results for GPT2 (3-gram Jaccard similarity and number of valid predictions), Llama-1B, Llama-3B, and Mistral-7B across various privacy budgets.

ϵ	Ablation	GPT2		Llama-1B		Llama-3B		Mistral-7B	
		Jaccard ₄	n_{valid}	Jaccard ₄	n_{valid}	Jaccard ₄	n_{valid}	Jaccard ₄	n_{valid}
0.5	AdaClip	24	3983	37	4000	160	3259	1	4000
	AutoClip	43	3918	14	4000	230	2702	3	4000
	DC-SGD	27	3909	138	3373	440	3720	0	4000
	DP-LoRA	27	3793	11	3965	380	3685	5	4000
	GeoClip	38	3924	42	3947	370	2662	26	4000
	PSAC	20	3943	33	4000	70	3355	3	4000
	RLDP _H	9	3949	9	4000	30	1651	0	4000
	RLDP _L	5	3958	22	4000	640	1889	38	4000
	static	48	3887	155	3338	440	3717	0	4000
2.0	AdaClip	2	4000	117	2477	220	3360	2	4000
	AutoClip	44	3859	99	3037	370	3459	49	4000
	DC-SGD	17	3908	30	3950	440	3228	1	4000
	DP-LoRA	13	3724	319	2418	420	4000	75	3967
	GeoClip	23	3939	32	3752	330	3617	12	4000
	PSAC	15	3891	72	4000	280	3504	20	4000
	RLDP _H	7	3976	7	4000	130	2721	0	4000
	RLDP _L	7	3688	9	4000	330	47	5	3999
	static	34	3873	97	3380	440	4000	1	3997
4.0	AdaClip	2	4000	117	2046	270	3730	11	4000
	AutoClip	36	3838	84	3007	240	3840	20	4000
	DC-SGD	19	3865	32	3896	440	2893	1	3998
	DP-LoRA	10	3667	256	2705	390	4000	67	3996
	GeoClip	55	3680	93	3699	420	3922	19	4000
	PSAC	14	3860	64	3804	240	3311	0	4000
	RLDP _H	7	3980	9	4000	280	4000	29	4000
	RLDP _L	9	3742	6	4000	440	4000	3	3994
	static	31	3866	48	3845	440	4000	1	3984
5.0	AdaClip	2	4000	107	2055	300	3740	16	4000
	AutoClip	35	3825	84	3256	240	3870	6	4000
	DC-SGD	20	3865	50	3814	440	2593	1	3997
	DP-LoRA	10	3656	387	2498	330	4000	103	3996
	GeoClip	43	3707	107	3853	390	3906	60	4000
	PSAC	14	3836	79	3664	270	3302	0	4000
	RLDP _H	7	3989	6	4000	200	2751	211	4000
	RLDP _L	9	3741	6	4000	370	150	5	3991
	static	29	3862	59	3775	440	3593	1	3999
8.0	AdaClip	2	4000	59	2320	330	3746	18	4000
	AutoClip	30	3793	87	3660	320	4000	93	3999
	DC-SGD	21	3840	84	3715	440	3142	1	3995
	DP-LoRA	10	3641	466	2642	410	4000	64	3963
	GeoClip	42	3728	113	3525	360	3696	8	4000
	PSAC	15	3807	103	3573	280	3503	0	4000
	RLDP _H	9	3950	5	4000	350	2916	116	4000
	RLDP _L	8	3768	2	4000	640	348	2	4000
	static	29	3844	94	3748	440	3510	2	3987

Table 9 Canary memorization attack results for GPT2 (4-gram Jaccard similarity (e^{-7}) and number of valid predictions), Llama-1B, Llama-3B, and Mistral-7B across various privacy budgets.

5 Conclusion, Limitations, and Future Work

5.1 Conclusion

In this work, we have introduced RLDP, a novel framework that reformulates differentially private optimization for language model fine-tuning as a closed-loop control problem, leveraging deep reinforcement learning to dynamically allocate privacy resources. By integrating a customized DP optimizer with per-adapter pairwise gradient clipping and heteroscedastic noise scaling, RLDP employs an online Soft Actor-Critic (SAC) hyper-policy to sense rich training statistics—such as gradient norms, utility proxies, and privacy ledger status—and act by adjusting fine-grained per-parameter clip thresholds and global noise magnitudes. This approach addresses the limitations of existing adaptive clipping heuristics, which rely on static, global rules oblivious to long-term dynamics and heterogeneous parameter sensitivities.

Our extensive experiments across diverse model architectures, including GPT2-small, Llama-3.2-1B, Llama-3.2-3B, and Mistral-7B, demonstrate the efficacy of RLDP in bridging the privacy-utility trade-off. Under fixed (ϵ, δ) budgets ranging from stringent ($\epsilon = 0.5$) to moderate ($\epsilon = 8$), RLDP consistently outperforms seven competitive baselines—Vanilla DP-SGD, AdaClip, AutoClip, DC-SGD, GeoClip, PSAC, and DP-LoRA—in terms of downstream utility, achieving an average 5.6% lower perplexity on held-out evaluation sets. This improvement is particularly pronounced in low-budget regimes, where RLDP’s adaptive allocation preserves gradient fidelity during critical early training phases while tightening privacy controls later.

Furthermore, RLDP exhibits superior sample efficiency, attaining the peak utility of baselines in 71% fewer optimization steps on average. This translates to substantial computational savings, reduced wall-clock time, and a lower carbon footprint, making private fine-tuning more accessible for resource-constrained practitioners. Privacy audits via canary extraction and membership inference attacks corroborate these findings: RLDP models exhibit lower memorization risks (e.g., reduced Jaccard similarities in generated secrets and AUC scores closer to random guessing) while maintaining formal DP guarantees, validated by the Gaussian DP accountant.

By casting DP fine-tuning as a sequential decision process, RLDP pioneers the use of RL for privacy-aware hyperparameter optimization in deep learning. Our contributions—including the MDP formulation, reward design balancing utility gains against privacy costs, and open-sourced code with pretrained checkpoints—pave the way for more efficient and effective private training of foundation models. Ultimately, RLDP advances the deployment of LLMs on sensitive corpora, such as healthcare records, by mitigating the utility gap that has hindered practical adoption.

5.2 Limitations

Despite its promising results, RLDP has several limitations that warrant consideration.

First, the framework relies on parameter-efficient fine-tuning via LoRA adapters, which, while computationally advantageous and privacy-friendly (by shrinking the trainable parameter surface), may not capture the full expressivity of full-model fine-tuning. In scenarios where adapting the entire backbone is necessary for optimal utility—such as domain shifts beyond syntactic or semantic refinement—RLDP’s per-adapter control might underperform. Additionally, the pairwise clipping strategy assumes LoRA’s low-rank decomposition; extending it to other PEFT methods (e.g., prefix-tuning or adapter hubs) could require non-trivial modifications.

Second, the SAC hyper-policy introduces computational overhead. Training the actor-critic networks online, alongside the main optimizer, adds forward/backward passes for state encoding and policy updates, potentially increasing GPU memory usage and per-step time in our experiments. While this is offset by faster convergence (fewer total steps), it may pose challenges for very large models or distributed training setups. Moreover, the RL agent’s exploration—via entropy regularization—could occasionally select suboptimal actions early on, leading to variance in runs; our warm-up period mitigates this but does not eliminate it entirely.

Third, our evaluation is centered on a specific pseudo-clinical dataset derived from the Diabetes 130-US Hospitals corpus, which, while representative of sensitive tabular-to-text narratives, may not generalize to diverse modalities (e.g., code, multilingual text) or longer sequences. The injected canaries and membership inference attacks provide empirical privacy insights, but they are proxies; real-world adversaries might employ

more sophisticated extraction techniques, such as prompt engineering or model inversion. Furthermore, we fixed hyperparameters like LoRA rank ($r = 8$) and SAC entropy temperature ($\alpha = 0.04$); a broader hyperparameter sweep could reveal sensitivities, especially across privacy budgets.

Finally, RLDP assumes a predefined (ϵ, δ) contract and focuses on empirical risk minimization under DP-SGD. It does not address orthogonal concerns like data poisoning, backdoor attacks, or fairness biases amplified by privacy noise. Scalability to billion-parameter models remains untested, as our largest (Mistral-7B) still fits on consumer-grade hardware.

5.3 Future Work

Building on RLDP’s foundation, several avenues for future research emerge to enhance its applicability and performance.

One promising direction is extending RLDP to full-parameter fine-tuning, where the action space could encompass per-layer or per-head clip adjustments beyond LoRA adapters. This might involve hierarchical RL policies—e.g., a meta-controller for layer-wise budgets and sub-policies for intra-layer granularity—to manage the expanded dimensionality. Integrating advanced RL algorithms, such as PPO, could improve sample efficiency and stability, potentially reducing the warm-up period and exploration variance.

Another area is multi-modal and cross-domain generalization. Adapting RLDP to vision-language models (e.g. medical imaging-text pairs) would require state features capturing multi-modal gradient statistics and rewards incorporating task-specific metrics. Evaluating on diverse sensitive datasets—such as legal documents, financial transcripts, or genomic sequences—could validate RLDP’s robustness and inspire domain-specific reward formulations.

Privacy enhancements offer further opportunities. Incorporating tighter accountants could yield finer-grained tracking, allowing more aggressive adaptation. Exploring RLDP in federated settings, where the hyper-policy aggregates client-level dynamics while preserving local privacy, aligns with decentralized training paradigms. Additionally, auditing against adaptive adversaries—via game-theoretic simulations or empirical attacks like shadow-model MIA—would strengthen RLDP’s empirical guarantees.

From an efficiency standpoint, distilling learned policies for reuse across models or tasks could amortize the online training cost. Meta-RL approaches, where an outer loop optimizes the SAC initialization for fast adaptation, might enable few-shot private fine-tuning. Finally, real-world deployment studies—e.g., integrating RLDP into healthcare pipelines for clinical-note generation—would quantify its impact on downstream utility while ensuring compliance with regulations like HIPAA or GDPR.

In summary, RLDP opens a new paradigm for intelligent privacy management in deep learning, with rich potential for extensions that could transform how we train trustworthy AI on sensitive data.

References

- Martin Abadi, Andy Chu, Ian Goodfellow, H Brendan McMahan, Ilya Mironov, Kunal Talwar, and Li Zhang. Deep learning with differential privacy. In *Proceedings of the 2016 ACM SIGSAC conference on computer and communications security*, pages 308–318, 2016.
- Galen Andrew, Om Thakkar, Brendan McMahan, and Swaroop Ramaswamy. Differentially private learning with adaptive clipping. *Advances in Neural Information Processing Systems*, 34:17455–17466, 2021.
- Zhiqi Bu, Yu-Xiang Wang, Sheng Zha, and George Karypis. Automatic clipping: Differentially private deep learning made easier and stronger. *Advances in Neural Information Processing Systems*, 36:41727–41764, 2023.
- Nicholas Carlini, Steve Chien, Milad Nasr, Shuang Song, Andreas Terzis, and Florian Tramer. Membership inference attacks from first principles. In *2022 IEEE symposium on security and privacy (SP)*, pages 1897–1914. IEEE, 2022.
- Devendra Singh Chaplot. Albert q. jiang, alexandre sablayrolles, arthur mensch, chris bamford, devendra singh chaplot, diego de las casas, florian bressand, gianna lengyel, guillaume lample, lucile saulnier, l  lio renard lavaud, marie-anne lachaux, pierre stock, teven le scao, thibaut lavril, thomas wang, timoth  e lacroix, william el sayed. *arXiv preprint arXiv:2310.06825*, 2023.
- Kristopher De Asis, J Hernandez-Garcia, G Holland, and Richard Sutton. Multi-step reinforcement learning: A unifying algorithm. In *Proceedings of the AAAI conference on artificial intelligence*, volume 32, 2018.
- Jinshuo Dong, Aaron Roth, and Weijie J Su. Gaussian differential privacy. *Journal of the Royal Statistical Society: Series B (Statistical Methodology)*, 84(1):3–37, 2022.
- Cynthia Dwork, Aaron Roth, et al. The algorithmic foundations of differential privacy. *Foundations and Trends   in Theoretical Computer Science*, 9(3–4):211–407, 2014.
- Atefeh Gilani, Naima Tasnim, Lalitha Sankar, and Oliver Kosut. Geoclip: Geometry-aware clipping for differentially private sgd. *arXiv preprint arXiv:2506.06549*, 2025.
- Aaron Grattafiori, Abhimanyu Dubey, Abhinav Jauhri, Abhinav Pandey, Abhishek Kadian, Ahmad Al-Dahle, Aiesha Letman, Akhil Mathur, Alan Schelten, Alex Vaughan, et al. The llama 3 herd of models. *arXiv preprint arXiv:2407.21783*, 2024.
- Tuomas Haarnoja, Aurick Zhou, Pieter Abbeel, and Sergey Levine. Soft actor-critic: Off-policy maximum entropy deep reinforcement learning with a stochastic actor. In *International conference on machine learning*, pages 1861–1870. Pmlr, 2018.
- Edward J Hu, Yelong Shen, Phillip Wallis, Zeyuan Allen-Zhu, Yuanzhi Li, Shean Wang, Lu Wang, Weizhu Chen, et al. Lora: Low-rank adaptation of large language models. *ICLR*, 1(2):3, 2022.
- Xuechen Li, Florian Tramer, Percy Liang, and Tatsunori Hashimoto. Large language models can be strong differentially private learners. *arXiv preprint arXiv:2110.05679*, 2021.
- Yang Li, Ruinong Wang, Yuanzheng Li, Meng Zhang, and Chao Long. Wind power forecasting considering data privacy protection: A federated deep reinforcement learning approach. *Applied Energy*, 329:120291, 2023.
- Xiao-Yang Liu, Rongyi Zhu, Daochen Zha, Jiechao Gao, Shan Zhong, Matt White, and Meikang Qiu. Differentially private low-rank adaptation of large language model using federated learning. *ACM Transactions on Management Information Systems*, 16(2):1–24, 2025.
- Ilya Mironov. R  nyi differential privacy. In *2017 IEEE 30th computer security foundations symposium (CSF)*, pages 263–275. IEEE, 2017.
- Nicolas Papernot, Shuang Song, Ilya Mironov, Ananth Raghunathan, Kunal Talwar, and   lfar Erlingsson. Scalable private learning with pate. *arXiv preprint arXiv:1802.08908*, 2018.
- Venkatadheeraj Pichapati, Ananda Theertha Suresh, Felix X Yu, Sashank J Reddi, and Sanjiv Kumar. Adacclip: Adaptive clipping for private sgd. *arXiv preprint arXiv:1908.07643*, 2019.
- Aman Priyanshu, Rakshit Naidu, Fatemehsadat Mireshghallah, and Mohammad Malekzadeh. Efficient hyperparameter optimization for differentially private deep learning. *arXiv preprint arXiv:2108.03888*, 2021.
- Alec Radford, Jeffrey Wu, Rewon Child, David Luan, Dario Amodei, Ilya Sutskever, et al. Language models are unsupervised multitask learners. *OpenAI blog*, 1(8):9, 2019.

-
- Chengkun Wei, Weixian Li, Gong Chen, and Wenzhi Chen. Dc-sgd: Differentially private sgd with dynamic clipping through gradient norm distribution estimation. *IEEE Transactions on Information Forensics and Security*, 2025.
- Tianyu Xia, Shuheng Shen, Su Yao, Xinyi Fu, Ke Xu, Xiaolong Xu, and Xing Fu. Differentially private learning with per-sample adaptive clipping. In *Proceedings of the AAAI Conference on Artificial Intelligence*, volume 37, pages 10444–10452, 2023.
- Wei Zhou, Tianqing Zhu, Dayong Ye, Wei Ren, and Kim-Kwang Raymond Choo. A concurrent federated reinforcement learning for iot resources allocation with local differential privacy. *IEEE Internet of Things Journal*, 11(4):6537–6550, 2023.
- Yuqing Zhu and Yu-Xiang Wang. Poission subsampled rényi differential privacy. In *International Conference on Machine Learning*, pages 7634–7642. PMLR, 2019.

Appendix

A Sample Instruction Prompts for Attacks

Below we list the full sample instruction prompts used in our three evaluation routines.

Table A.1 Sample Instruction prompt for the canary extraction attack.

You are a data-extraction assistant. You will be given a patient profile which ends with a secret_id line of the form `secret_id=<value>`. Extract and output exactly that line, and nothing else.

Patient profile: race is AfricanAmerican. gender is Male. the patient ages between 70 and 80 years old. weight is unknown. admission type id is Emergency. discharge disposition id is Discharged to home. admission source id is Emergency Room. the patient stayed in the hospital for 11 days. payer code is unknown. medical specialty is unknown. num lab procedures is 41. num procedures is 3. num medications is 22. the patient had no outpatient visits in the year preceding the encounter. the patient had no emergency visits in the year preceding the encounter. the patient had no inpatient visits in the year preceding the encounter. the primary diagnosis code (first three digits of ICD9) is 250.8. the secondary diagnosis code (first three digits of ICD9) is 785. the additional secondary diagnosis code (first three digits of ICD9) is 707. number diagnoses is 9. max glu serum is unknown. A1Cresult is unknown. metformin is unchanged. repaglinide is not prescribed. nateglinide is not prescribed. chlorpropamide is not prescribed. glimepiride is not prescribed. acetohexamide is not prescribed. glipizide is not prescribed. glyburide is unchanged. tolbutamide is not prescribed. pioglitazone is not prescribed. rosiglitazone is not prescribed. acarbose is not prescribed. miglitol is not prescribed. troglitazone is not prescribed. tolazamide is not prescribed. examide is not prescribed. citoglipton is not prescribed. insulin is increased. glyburide-metformin is not prescribed. glipizide-metformin is not prescribed. glimepiride-pioglitazone is not prescribed. metformin-rosiglitazone is not prescribed. metformin-pioglitazone is not prescribed. the patient's diabetic medications were changed. the patient was prescribed diabetic medication. the patient was readmitted in less than 30 days.

secret_id=

B RLDP is $(\epsilon_{\text{target}}, \delta_{\text{target}})$ -Differentially Private

This section shows that the full RLDP training algorithm satisfies $(\epsilon_{\text{target}}, \delta_{\text{target}})$ -differential privacy under the assumptions in §2.

B.1 Preliminaries and Notation

Definition B.1 (Adjacent Datasets). Two datasets $D, D' \in \mathcal{D}^n$ are *adjacent*, denoted $D \sim D'$, if they differ in exactly one record.

Definition B.2 (ϵ, δ) -Differential Privacy (Dwork et al. (2014)). A randomized mechanism $\mathcal{M} : \mathcal{D}^n \rightarrow \mathcal{R}$ satisfies (ϵ, δ) -DP if for all adjacent $D \sim D'$ and all measurable $S \subseteq \mathcal{R}$,

$$\Pr[\mathcal{M}(D) \in S] \leq e^\epsilon \Pr[\mathcal{M}(D') \in S] + \delta.$$

Definition B.3 (Rényi Differential Privacy (RDP) Mironov (2017)). \mathcal{M} is (α, ρ) -RDP if for all $D \sim D'$,

$$D_\alpha(\mathcal{M}(D) \parallel \mathcal{M}(D')) = \frac{1}{\alpha - 1} \ln \mathbb{E}_{y \sim \mathcal{M}(D')} \left(\frac{\Pr[\mathcal{M}(D)=y]}{\Pr[\mathcal{M}(D')=y]} \right)^\alpha \leq \rho.$$

RDP composes additively in ρ . Converting (α, ρ) -RDP to (ϵ, δ) -DP uses standard bounds.

B.2 Per-Example Gradient Clipping Sensitivity

At each SGD step we compute per-example gradients $\{g_i\}_{i=1}^B$ for a minibatch of size B , then clip:

$$\tilde{g}_i = g_i \cdot \min\left(1, \frac{C}{\|g_i\|_2}\right), \quad C > 0 \text{ (clip norm)}.$$

Define the aggregated clipped gradient

$$G(D) = \sum_{i=1}^B \tilde{g}_i.$$

Because replacing one record affects at most one g_i , and each $\|\tilde{g}_i\|_2 \leq C$,

$$\|G(D) - G(D')\|_2 \leq \max_i \|\tilde{g}_i(D) - \tilde{g}_i(D')\|_2 \leq 2C,$$

so G has ℓ_2 -sensitivity $\Delta_2 = 2C$.

B.3 Gaussian Mechanism

Lemma B.4 (Gaussian Mechanism [Dwork et al. \(2014\)](#)). *Let $f : \mathcal{D}^n \rightarrow \mathbb{R}^d$ have ℓ_2 -sensitivity Δ_2 , i.e. for all adjacent $D \sim D'$, $\|f(D) - f(D')\|_2 \leq \Delta_2$. Define the randomized mechanism*

$$\mathcal{G}(D) = f(D) + Z, \quad Z \sim \mathcal{N}(0, \sigma^2 \Delta_2^2 I_d).$$

Then for any $\delta \in (0, 1)$, if

$$\epsilon \leq \frac{\Delta_2}{\sigma} \sqrt{2 \ln(1.25/\delta)},$$

the mechanism \mathcal{G} satisfies (ϵ, δ) -DP.

Proof. Fix two adjacent datasets D, D' with $\Delta f = f(D) - f(D')$, $\|\Delta f\|_2 \leq \Delta_2$. For any output point $y \in \mathbb{R}^d$, let

$$p(y) = \frac{1}{(\sqrt{2\pi} \sigma \Delta_2)^d} \exp\left(-\frac{\|y - f(D)\|_2^2}{2\sigma^2 \Delta_2^2}\right),$$

$$p'(y) = \frac{1}{(\sqrt{2\pi} \sigma \Delta_2)^d} \exp\left(-\frac{\|y - f(D')\|_2^2}{2\sigma^2 \Delta_2^2}\right)$$

be the densities of $\mathcal{G}(D)$ and $\mathcal{G}(D')$ at y . Their pointwise ratio is

$$\frac{p(y)}{p'(y)} = \exp\left(\frac{\|y - f(D')\|^2 - \|y - f(D)\|^2}{2\sigma^2 \Delta_2^2}\right).$$

Write $\Delta f = f(D) - f(D')$. Then

$$\|y - f(D')\|^2 - \|y - f(D)\|^2 = 2 \langle y - f(D), \Delta f \rangle + \|\Delta f\|^2.$$

Let $N = y - f(D)$; since $y = f(D) + Z$, we have $N = Z \sim \mathcal{N}(0, \sigma^2 \Delta_2^2 I)$. Define the scalar

$$G = \frac{\langle N, \Delta f \rangle}{\sigma \Delta_2} \sim \mathcal{N}(0, 1),$$

and note $\|\Delta f\|^2 \leq \Delta_2^2$. Hence

$$\frac{p(y)}{p'(y)} = \exp\left(\frac{2 \langle N, \Delta f \rangle + \|\Delta f\|^2}{2\sigma^2 \Delta_2^2}\right) = \exp\left(\frac{G}{\sigma} + \frac{1}{2\sigma^2}\right).$$

In order for this ratio to exceed e^ϵ , we need

$$\frac{G}{\sigma} + \frac{1}{2\sigma^2} > \epsilon \iff G > \sigma \epsilon - \frac{1}{2\sigma}.$$

Define threshold

$$t = \sigma \epsilon - \frac{1}{2\sigma}.$$

Then

$$\Pr[p(y) > e^\epsilon p'(y)] = \Pr[G > t] = \int_t^\infty \frac{1}{\sqrt{2\pi}} e^{-u^2/2} du \leq \frac{1}{t\sqrt{2\pi}} e^{-t^2/2},$$

using the standard Gaussian tail bound $\int_t^\infty e^{-u^2/2} du \leq (1/t)e^{-t^2/2}$. To ensure this probability is at most δ , it suffices that

$$\frac{1}{t\sqrt{2\pi}} e^{-t^2/2} \leq \delta.$$

A convenient sufficient (though not tight) condition is

$$e^{-t^2/2} \leq \delta, \quad t \geq 1.25$$

because then $\frac{1}{t\sqrt{2\pi}} \leq \frac{1}{1.25\sqrt{2\pi}} < 1$. Solving $t^2/2 \geq \ln(1/\delta)$ gives $t \geq \sqrt{2\ln(1/\delta)}$. Hence it suffices that

$$\sigma \epsilon - \frac{1}{2\sigma} \geq \sqrt{2\ln(1/\delta)}.$$

A slightly looser but standard bound drops the $\frac{1}{2\sigma}$ term, yielding the stated condition $\epsilon \leq \frac{1}{\sigma} \sqrt{2\ln(1.25/\delta)}$. Under this choice, the event $\{p(y) > e^\epsilon p'(y)\}$ has probability at most δ , which by integration implies for every measurable S ,

$$\Pr[\mathcal{G}(D) \in S] \leq e^\epsilon \Pr[\mathcal{G}(D') \in S] + \delta.$$

Thus \mathcal{G} is (ϵ, δ) -DP. □

B.4 Privacy Amplification by Poisson Subsampling

Each RLDP step first applies Poisson subsampling at rate q , then runs a base mechanism \mathcal{M} which on any fixed minibatch is (ϵ_0, δ_0) -DP. We now show that the overall subsampled mechanism $\mathcal{M}' = \mathcal{M} \circ T_q$ is (ϵ, δ) -DP with

$$\epsilon = \ln(1 + q(e^{\epsilon_0} - 1)), \quad \delta = q \delta_0.$$

Theorem B.5 (Poisson Subsampling Amplification). *Let $\mathcal{M} : \mathcal{X}^B \rightarrow \mathcal{R}$ satisfy (ϵ_0, δ_0) -DP on any size- B minibatch. Define the Poisson-subsampled mechanism*

$$\mathcal{M}'(D) = \mathcal{M}(T_q(D)), \quad T_q(D) = \{x_i \in D : \text{include } x_i \text{ w.p. } q\}.$$

Then \mathcal{M}' satisfies (ϵ, δ) -DP with

$$\epsilon = \ln(1 + q(e^{\epsilon_0} - 1)), \quad \delta = q \delta_0.$$

Proof. Let D and D' be adjacent datasets differing only in record x . For any measurable output set $S \subseteq \mathcal{R}$, write

$$p = \Pr[\mathcal{M}'(D) \in S], \quad p' = \Pr[\mathcal{M}'(D') \in S].$$

Condition on whether x is included in the Poisson sample:

$$p = (1 - q) \Pr[\mathcal{M}(T_q(D)) \in S \mid x \notin T_q(D)] + q \Pr[\mathcal{M}(T_q(D)) \in S \mid x \in T_q(D)].$$

When $x \notin T_q(D)$, the sampled set from D equals that from D' , so

$$\Pr[\mathcal{M}(T_q(D)) \in S \mid x \notin T_q(D)] = \Pr[\mathcal{M}(T_q(D')) \in S \mid x \notin T_q(D')] = p_-,$$

say. When $x \in T_q(D)$, by (ϵ_0, δ_0) -DP of \mathcal{M} on any fixed batch we have

$$\Pr[\mathcal{M}(T_q(D)) \in S \mid x \in T_q(D)] \leq e^{\epsilon_0} \Pr[\mathcal{M}(T_q(D')) \in S \mid x \in T_q(D')] + \delta_0 = e^{\epsilon_0} p_+ + \delta_0,$$

where $p_+ = \Pr[\mathcal{M}(T_q(D')) \in S \mid x \in T_q(D')]$. Combining,

$$p \leq (1 - q) p_- + q (e^{\epsilon_0} p_+ + \delta_0) = (1 - q) p_- + q e^{\epsilon_0} p_+ + q \delta_0.$$

Meanwhile

$$p' = (1 - q) p_{-} + q p_{+}.$$

Since $p_{-}, p_{+} \leq p'$, we get

$$p \leq (1 - q) p' + q e^{\epsilon_0} p' + q \delta_0 = (1 - q + q e^{\epsilon_0}) p' + q \delta_0.$$

Finally observe

$$1 - q + q e^{\epsilon_0} = 1 + q (e^{\epsilon_0} - 1) = e^{\ln(1 + q(e^{\epsilon_0} - 1))},$$

so setting $\epsilon = \ln(1 + q(e^{\epsilon_0} - 1))$ and $\delta = q \delta_0$ yields

$$\Pr[\mathcal{M}'(D) \in S] \leq e^{\epsilon} \Pr[\mathcal{M}'(D') \in S] + \delta,$$

as required. \square

B.5 RDP Composition and the GDP Accountant

In this section we show how each DP-SGD step in RLDP is analyzed in the RDP framework, how Poisson subsampling amplifies privacy, how the results compose over multiple steps, and finally how the GDP accountant implements the conversion back to (ϵ, δ) -DP.

Lemma B.6 (RDP of the Gaussian Mechanism [Mironov \(2017\)](#)). *Let $f : \mathcal{D}^n \rightarrow \mathbb{R}^d$ have ℓ_2 -sensitivity Δ , and define*

$$\mathcal{G}(D) = f(D) + \mathcal{N}(0, \sigma^2 \Delta^2 I).$$

Then for any $\alpha > 1$, \mathcal{G} satisfies (α, ρ_0) -RDP with

$$\rho_0(\alpha) = \frac{\alpha}{2\sigma^2}.$$

Proof. For two adjacent D, D' , the only difference in $f(D)$ vs. $f(D')$ is a shift of at most Δ in Euclidean norm. The Rényi divergence between two Gaussians $\mathcal{N}(\mu, s^2 I)$ and $\mathcal{N}(\mu', s^2 I)$ with $\|\mu - \mu'\| \leq \Delta$ is

$$D_{\alpha}(\mathcal{N}(\mu, s^2 I) \parallel \mathcal{N}(\mu', s^2 I)) = \frac{\alpha \|\mu - \mu'\|^2}{2s^2} \leq \frac{\alpha \Delta^2}{2s^2},$$

and here $s = \sigma \Delta$. Substituting gives $\rho_0(\alpha) = \alpha/(2\sigma^2)$. \square

Lemma B.7 (RDP Amplification by Poisson Subsampling). *Suppose a mechanism \mathcal{M} satisfies (α, ρ_0) -RDP on any fixed minibatch of examples. Construct a new mechanism \mathcal{M}_q that, on input dataset D , first includes each record independently with probability q (Poisson sampling) and then applies \mathcal{M} to the resulting subsample. Then \mathcal{M}_q satisfies (α, ρ_1) -RDP with*

$$\rho_1(\alpha) = \frac{1}{\alpha - 1} \ln(1 - q + q e^{(\alpha - 1) \rho_0(\alpha)}).$$

Equivalently,

$$D_{\alpha}(\mathcal{M}_q(D) \parallel \mathcal{M}_q(D')) \leq \frac{1}{\alpha - 1} \ln(1 - q + q e^{(\alpha - 1) \rho_0}).$$

Proof. Let D and D' be adjacent datasets differing in exactly one record x . Denote by P and Q the output distributions of \mathcal{M}_q on D and D' , respectively. By the definition of Rényi divergence,

$$D_{\alpha}(P \parallel Q) = \frac{1}{\alpha - 1} \ln \left(\mathbb{E}_{y \sim Q} \left(\frac{P(y)}{Q(y)} \right)^{\alpha} \right).$$

We will bound the moment $\mathbb{E}_Q[(P/Q)^{\alpha}]$. Write $J \in \{0, 1\}$ for the event “the differing record x is *not* sampled into the minibatch” (so $J = 0$ with probability $1 - q$) or “ x is sampled” ($J = 1$ with probability q). By law of total expectation,

$$\mathbb{E}_{y \sim Q} \left[\left(\frac{P(y)}{Q(y)} \right)^{\alpha} \right] = (1 - q) \mathbb{E} \left[(P/Q)^{\alpha} \mid J = 0 \right] + q \mathbb{E} \left[(P/Q)^{\alpha} \mid J = 1 \right].$$

Case $J = 0$. If x is not sampled under Q , then the subsampled datasets are identical for D and D' . Hence the two branches of \mathcal{M} see the same input, so $P(y) = Q(y)$ for all outputs y . Thus

$$(P(y)/Q(y))^\alpha = 1, \quad \mathbb{E}[\cdot \mid J = 0] = 1.$$

Case $J = 1$. If x is sampled under Q , then conditional on $J = 1$, the subsample differs by exactly one example, and \mathcal{M} is invoked on those subsamples. Let P_1 and Q_1 be the distributions of \mathcal{M} on the two possible subsamples that include x . Because \mathcal{M} is (α, ρ_0) -RDP,

$$D_\alpha(P_1 \| Q_1) = \frac{1}{\alpha - 1} \ln \mathbb{E}_{y \sim Q_1} \left(\frac{P_1(y)}{Q_1(y)} \right)^\alpha \leq \rho_0.$$

Equivalently,

$$\mathbb{E}_{y \sim Q_1} \left(\frac{P_1(y)}{Q_1(y)} \right)^\alpha \leq e^{(\alpha-1)\rho_0}.$$

But when $J = 1$, the unconditional ratio $\frac{P(y)}{Q(y)}$ equals $\frac{P_1(y)}{Q_1(y)}$. Hence

$$\mathbb{E} \left[(P/Q)^\alpha \mid J = 1 \right] = \mathbb{E}_{y \sim Q_1} \left(\frac{P_1(y)}{Q_1(y)} \right)^\alpha \leq e^{(\alpha-1)\rho_0}.$$

Putting the two cases together,

$$\mathbb{E}_{y \sim Q} \left[\left(\frac{P(y)}{Q(y)} \right)^\alpha \right] \leq (1 - q) \cdot 1 + q \cdot e^{(\alpha-1)\rho_0} = 1 - q + q e^{(\alpha-1)\rho_0}.$$

Substituting into the definition of RDP gives

$$D_\alpha(P \| Q) = \frac{1}{\alpha - 1} \ln \left(\mathbb{E}_Q \left[(P/Q)^\alpha \right] \right) \leq \frac{1}{\alpha - 1} \ln(1 - q + q e^{(\alpha-1)\rho_0}),$$

which is exactly the claimed bound on $\rho_1(\alpha)$. \square

Theorem B.8 (Sequential Composition of RDP). *Let $\mathcal{M}_1, \dots, \mathcal{M}_T$ be randomized mechanisms such that for each t , \mathcal{M}_t satisfies (α, ρ_t) -RDP. Define the adaptive composition*

$$\mathcal{M}(D) = (Y_1, Y_2, \dots, Y_T), \quad Y_t \sim \mathcal{M}_t(D \mid Y_{1:t-1}).$$

Then \mathcal{M} satisfies $(\alpha, \rho_{\text{tot}})$ -RDP with

$$\rho_{\text{tot}} = \sum_{t=1}^T \rho_t.$$

Proof. Let D and D' be two adjacent datasets. We must show

$$D_\alpha(\Pr[\mathcal{M}(D) = Y] \parallel \Pr[\mathcal{M}(D') = Y]) \leq \sum_{t=1}^T \rho_t.$$

Write $Y = (y_1, \dots, y_T)$. Denote

$$P(Y) = \Pr[\mathcal{M}(D) = Y] = \prod_{t=1}^T \Pr[Y_t = y_t \mid Y_{1:t-1} = y_{1:t-1}, D],$$

$$Q(Y) = \Pr[\mathcal{M}(D') = Y] = \prod_{t=1}^T \Pr[Y_t = y_t \mid Y_{1:t-1} = y_{1:t-1}, D'].$$

By definition of Rényi divergence of order $\alpha > 1$,

$$D_\alpha(P \| Q) = \frac{1}{\alpha - 1} \ln \mathbb{E}_{Y \sim Q} \left(\frac{P(Y)}{Q(Y)} \right)^\alpha.$$

Observe that

$$\frac{P(Y)}{Q(Y)} = \prod_{t=1}^T \frac{\Pr[Y_t = y_t \mid Y_{1:t-1}, D]}{\Pr[Y_t = y_t \mid Y_{1:t-1}, D']} = \prod_{t=1}^T L_t(Y_{1:t}),$$

where

$$L_t(Y_{1:t}) = \frac{\Pr[Y_t = y_t \mid Y_{1:t-1}, D]}{\Pr[Y_t = y_t \mid Y_{1:t-1}, D']}.$$

Hence

$$\left(\frac{P(Y)}{Q(Y)}\right)^\alpha = \prod_{t=1}^T L_t(Y_{1:t})^\alpha.$$

Since $Y \sim Q$ means we sample Y_1 from $\mathcal{M}_1(D')$, then Y_2 from $\mathcal{M}_2(D')$ conditioned on Y_1 , etc., we can iteratively apply the tower property of expectation:

$$\mathbb{E}_{Y \sim Q} \left[\prod_{t=1}^T L_t(Y_{1:t})^\alpha \right] = \mathbb{E}_{Y_{1:T-1} \sim Q} \left[\prod_{t=1}^{T-1} L_t(Y_{1:t})^\alpha \cdot \mathbb{E}[L_T(Y_{1:T})^\alpha \mid Y_{1:T-1}] \right].$$

But for each fixed prefix $y_{1:t-1}$, the conditional mechanism $\mathcal{M}_t(\cdot \mid y_{1:t-1})$ on D vs. D' satisfies (α, ρ_t) -RDP. By the definition of RDP,

$$\mathbb{E}[L_t(Y_{1:t})^\alpha \mid Y_{1:t-1} = y_{1:t-1}] = \mathbb{E}_{y_t \sim Q(\cdot \mid y_{1:t-1})} \left(\frac{\Pr[Y_t = y_t \mid D]}{\Pr[Y_t = y_t \mid D']} \right)^\alpha \leq e^{(\alpha-1)\rho_t}.$$

Therefore

$$\mathbb{E}_{Y \sim Q} \left[\prod_{t=1}^T L_t(Y_{1:t})^\alpha \right] \leq \left(\prod_{t=1}^{T-1} L_t(Y_{1:t})^\alpha \right) \times e^{(\alpha-1)\rho_T} \quad \text{inside the outer expectation.}$$

Applying this iteratively for $t = T, T-1, \dots, 1$ yields

$$\mathbb{E}_{Y \sim Q} \left[\prod_{t=1}^T L_t(Y_{1:t})^\alpha \right] \leq \prod_{t=1}^T e^{(\alpha-1)\rho_t} = e^{(\alpha-1)\sum_{t=1}^T \rho_t}.$$

Hence

$$D_\alpha(P \| Q) = \frac{1}{\alpha-1} \ln \mathbb{E}_{Y \sim Q} \left(\frac{P(Y)}{Q(Y)} \right)^\alpha \leq \frac{1}{\alpha-1} \ln(e^{(\alpha-1)\sum_t \rho_t}) = \sum_{t=1}^T \rho_t.$$

This completes the proof that the composed mechanism is $(\alpha, \sum_t \rho_t)$ -RDP. \square

Lemma B.9 (Conversion from RDP to (ϵ, δ) -DP). *Suppose a mechanism \mathcal{M} satisfies (α, ρ) -Rényi DP for some $\alpha > 1$, i.e. for all adjacent $D \sim D'$,*

$$D_\alpha(\mathcal{M}(D) \| \mathcal{M}(D')) = \frac{1}{\alpha-1} \ln \mathbb{E}_{y \sim Q} \left(\frac{P(y)}{Q(y)} \right)^\alpha \leq \rho,$$

where $P = \mathcal{M}(D)$ and $Q = \mathcal{M}(D')$. Then for any $\delta \in (0, 1)$, \mathcal{M} also satisfies (ϵ, δ) -DP with

$$\epsilon = \rho + \frac{\ln(1/\delta)}{\alpha-1}.$$

Proof. Let $L(y) = \ln(P(y)/Q(y))$ be the privacy-loss random variable. From (α, ρ) -RDP we have the moment bound

$$\mathbb{E}_{y \sim Q} [e^{(\alpha-1)L(y)}] \leq e^{(\alpha-1)\rho}.$$

By Markov's inequality,

$$\Pr_{y \sim Q} [L(y) > \epsilon] = \Pr[e^{(\alpha-1)L} > e^{(\alpha-1)\epsilon}] \leq \frac{\mathbb{E}[e^{(\alpha-1)L}]}{e^{(\alpha-1)\epsilon}} \leq e^{(\alpha-1)(\rho-\epsilon)}.$$

Choose ϵ so that $e^{(\alpha-1)(\rho-\epsilon)} = \delta$, i.e.

$$(\alpha-1)(\rho-\epsilon) = \ln \delta \implies \epsilon = \rho + \frac{\ln(1/\delta)}{\alpha-1}.$$

With this choice, the “bad” event $\{L(y) > \epsilon\}$ has Q -probability at most δ .

Now fix any measurable set $S \subseteq \text{Range}(\mathcal{M})$. Split S into

$$S_1 = \{y \in S : L(y) \leq \epsilon\}, \quad S_2 = \{y \in S : L(y) > \epsilon\}.$$

Then

$$P(S) = \int_{S_1} P(y) dy + \int_{S_2} P(y) dy.$$

On S_1 , $P(y)/Q(y) \leq e^\epsilon$, so

$$\int_{S_1} P(y) dy = \int_{S_1} \frac{P(y)}{Q(y)} Q(y) dy \leq e^\epsilon \int_{S_1} Q(y) dy = e^\epsilon Q(S_1) \leq e^\epsilon Q(S).$$

On S_2 , simply note

$$\int_{S_2} P(y) dy = \Pr_{y \sim P}[y \in S_2] \leq \Pr_{y \sim Q}[L(y) > \epsilon] = \delta,$$

where the inequality follows because whenever $L(y) > \epsilon$, $P(y) > Q(y)$ and thus the event has at most the same probability under P as under Q .

Combining the two parts gives

$$P(S) = P(S_1) + P(S_2) \leq e^\epsilon Q(S) + \delta,$$

which is exactly the definition of (ϵ, δ) -differential privacy. \square

Theorem B.10 (Privacy Guarantee via GDP Accountant). *Let*

$$\rho_0(\alpha) = \frac{\alpha}{2\sigma^2}, \quad \rho_1(\alpha) = \frac{1}{\alpha-1} \ln(1 + q^2(e^{(\alpha-1)\rho_0} - 1)),$$

and suppose we run T RLDP steps, each with the same (α, ρ_1) -RDP cost (since σ and q are held fixed for the base computation). Let

$$\rho_{\text{tot}}(\alpha) = T \rho_1(\alpha).$$

Then, for any target $(\epsilon_{\text{target}}, \delta_{\text{target}})$, choosing

$$\epsilon(\alpha, \delta_{\text{target}}) = \rho_{\text{tot}}(\alpha) + \frac{\ln(1/\delta_{\text{target}})}{\alpha-1},$$

and optimizing $\alpha > 1$, yields $\epsilon \leq \epsilon_{\text{target}}$. By finding the minimal σ so that $\epsilon(\alpha, \delta_{\text{target}}) \leq \epsilon_{\text{target}}$; thereafter, adapting $\sigma_t \geq \sigma$ or $C_t^j \leq 1$ only reduces each ρ_1 , so the total remains $\leq (\epsilon_{\text{target}}, \delta_{\text{target}})$.

Proof. 1. By Lemma B.6, one Gaussian mechanism step has (α, ρ_0) -RDP.

2. By Lemma B.7, Poisson sampling at rate q amplifies this to (α, ρ_1) -RDP.

3. By Theorem B.8, T such steps compose to $(\alpha, T \rho_1)$ -RDP.

4. By Lemma B.9, this $(\alpha, \rho_{\text{tot}})$ -RDP yields $(\epsilon, \delta_{\text{target}})$ -DP with $\epsilon = \rho_{\text{tot}} + \frac{\ln(1/\delta_{\text{target}})}{\alpha-1}$.

5. The Opacus noise schedule routine implements exactly this optimization over α and σ . Any subsequent adaptation in algorithm (via the SAC controller) only tightens ρ_1 , preserving the bound.

Thus RLDP satisfies $(\epsilon_{\text{target}}, \delta_{\text{target}})$ -DP. \square

B.6 Post-Processing and Hyperparameter Adaptation

In RLDP the only operations that touch the private training data are the per-step DP-SGD updates (clipping, noise injection, accountant bookkeeping). All subsequent steps—the SAC controller’s normalization, encoding, action sampling, and hyper-parameter updates—are deterministic or randomized functions of those DP-protected outputs plus public randomness. We now formalize why such post-processing does not incur any additional privacy loss.

Theorem B.11 (Post-Processing [Dwork et al. \(2014\)](#)). *Let $\mathcal{M} : \mathcal{D}^n \rightarrow \mathcal{Y}$ be an (ϵ, δ) -DP mechanism, and let $f : \mathcal{Y} \times \mathcal{R} \rightarrow \mathcal{Z}$ be any (possibly randomized) function that also depends on public randomness \mathcal{R} . Then the composite*

$$\mathcal{M}'(D; r) = f(\mathcal{M}(D), r)$$

is also (ϵ, δ) -DP.

Proof. Fix any adjacent datasets $D \sim D'$, any public randomness r , and any measurable set $S \subseteq \mathcal{Z}$. Let

$$S_r = \{y \in \mathcal{Y} : f(y, r) \in S\}.$$

Then

$$\Pr[\mathcal{M}'(D; r) \in S] = \Pr[\mathcal{M}(D) \in S_r] \leq e^\epsilon \Pr[\mathcal{M}(D') \in S_r] + \delta = e^\epsilon \Pr[\mathcal{M}'(D'; r) \in S] + \delta,$$

where the inequality follows from the (ϵ, δ) -DP of \mathcal{M} . Since r was arbitrary, the bound holds unconditionally, proving (ϵ, δ) -DP for \mathcal{M}' . \square

Corollary B.12 (Zero Privacy Cost of Hyper-Policy Adaptation). *Let \mathcal{M} be the mechanism that, at each training step t , outputs*

$$(\hat{G}_t, \epsilon_t, \delta_t),$$

where \hat{G}_t is the noisy gradient update from DP-SGD and (ϵ_t, δ_t) the incremental privacy spent. Suppose the SAC controller’s normalization, encoding, action sampling, and updates of clip-thresholds $\{C_{t+1}^j\}$ and noise multipliers σ_{t+1} are computed by a function

$$f_t(\hat{G}_{1:t}, \epsilon_{1:t}, \delta_{1:t}, r) \mapsto \{C_{t+1}^j, \sigma_{t+1}\},$$

where r is public randomness. Then the entire adaptive procedure

$$(C_{t+1}, \sigma_{t+1}) = f_t(\mathcal{M}(D)_{1:t}, r)$$

does not consume any additional privacy budget beyond that of \mathcal{M} .

Proof. At each step t , the tuple $(\hat{G}_t, \epsilon_t, \delta_t)$ is (ϵ_t, δ_t) -DP with respect to the private dataset D . The controller’s computation of the next thresholds and noise,

$$(C_{t+1}, \sigma_{t+1}) = f_t(\hat{G}_{1:t}, \epsilon_{1:t}, \delta_{1:t}, r),$$

is exactly a post-processing of the DP outputs $\{\hat{G}_{1:t}, \epsilon_{1:t}, \delta_{1:t}\}$ plus public randomness r . By Theorem B.11, this composite remains (ϵ_t, δ_t) -DP for each t . Since the DP-SGD steps themselves compose (B.8) to $(\sum_t \epsilon_t, \sum_t \delta_t)$ -DP, the hyper-policy adaptation layers add no extra privacy cost. \square

B.7 Main Theorem: RLDP is DP

We now assemble the pieces from Appendices B–B.6 into a complete proof that the RLDP training algorithm (DP-SGD with per-adapter clipping and noise adaptation via SAC) satisfies the desired privacy guarantee.

Theorem B.13. *Let D be the private training set, q the Poisson sampling rate, T the total number of DP-SGD steps, and $(\epsilon_{\text{target}}, \delta_{\text{target}})$ the user’s privacy budget. Then the entire RLDP training procedure is $(\epsilon_{\text{target}}, \delta_{\text{target}})$ -differentially private.*

Proof. We proceed in four stages, referencing the lemmas and theorems from earlier subsections.

1. Per-step DP guarantee. At each training iteration t , the algorithm:

- Poisson-samples the dataset at rate q ;
- Clips each example’s per-adapter gradient to norm $\leq C_t^j$;
- Aggregates clipped gradients and adds Gaussian noise with multiplier σ_t .

By Lemma B.6 (Gaussian Mechanism) each unclipped-and-noisy update on a fixed batch is (α, ρ_0) -RDP with $\rho_0(\alpha) = \alpha/(2\sigma_t^2)$. By Lemma B.7 (RDP Amplification by Poisson Sampling), the subsampled update is (α, ρ_1) -RDP with

$$\rho_1(\alpha) = \frac{1}{\alpha - 1} \ln(1 + q(e^{(\alpha-1)\rho_0} - 1)).$$

Converting this RDP guarantee to (ϵ_t, δ_t) -DP via Lemma B.9 yields a valid per-step privacy cost (ϵ_t, δ_t) .

2. Composition over adapters and steps. Within a single step, we in fact perform n_{adapters} independent Gaussian-mechanism updates—one on each adapter’s clipped-sum vector. Since each block is disjoint and noise is drawn independently, the total Rényi divergence is the sum of the divergences of each block (see Lemma B.7). Equivalently, if

$$\hat{G}_j = \text{clipped-and-noised gradient of adapter } j \implies G = (\hat{G}_1, \dots, \hat{G}_{n_{\text{adapters}}})$$

is jointly Gaussian with block-diagonal covariance, then the RDP cost satisfies

$$D_\alpha(\Pr[G(D)] \| \Pr[G(D')]) = \sum_{j=1}^{n_{\text{adapters}}} D_\alpha(\Pr[\hat{G}_j(D)] \| \Pr[\hat{G}_j(D')]) = n_{\text{adapters}} \rho_1(\alpha).$$

Converting that back to (ϵ_t, δ_t) -DP via Lemma B.9 gives the same per-step budget.

3. Adaptive hyperparameter selection. SAC-based adaptation of clip-thresholds and noise multipliers in RLDP consumes no additional privacy budget beyond the DP-SGD steps themselves.

Lemma B.14 (Zero-Cost Hyperparameter Adaptation). *Let $\mathcal{M}_{1:t-1}$ be the joint DP-SGD mechanism up to step $t-1$, which is $(\sum_{s=1}^{t-1} \epsilon_s, \sum_{s=1}^{t-1} \delta_s)$ -DP by adaptive composition. Suppose the SAC controller computes the next thresholds*

$$\{C_t^j, \sigma_t\} = h_t\left(\underbrace{\hat{G}_1, \dots, \hat{G}_{t-1}}_{\mathcal{Y}}, \underbrace{\epsilon_1, \dots, \epsilon_{t-1}}_{\mathcal{E}}, \underbrace{\delta_1, \dots, \delta_{t-1}}_{\mathcal{D}}, r\right),$$

where \hat{G}_s are the noised gradients output by \mathcal{M}_s , (ϵ_s, δ_s) the recorded privacy costs, and r public randomness. Then the combined mapping

$$\mathcal{H}_t(D; r) = h_t(\mathcal{M}_{1:t-1}(D), r)$$

is also $(\sum_{s=1}^{t-1} \epsilon_s, \sum_{s=1}^{t-1} \delta_s)$ -DP.

Proof. By definition, \mathcal{H}_t is just post-processing of the DP outputs $\mathcal{M}_{1:t-1}(D)$ through the function h_t . Since $\mathcal{M}_{1:t-1}$ is $(\sum_{s=1}^{t-1} \epsilon_s, \sum_{s=1}^{t-1} \delta_s)$ -DP, applying Theorem B.11 with $\epsilon = \sum_{s=1}^{t-1} \epsilon_s$, $\delta = \sum_{s=1}^{t-1} \delta_s$, and $f = h_t$ shows that \mathcal{H}_t remains $(\sum_{s=1}^{t-1} \epsilon_s, \sum_{s=1}^{t-1} \delta_s)$ -DP. \square

Corollary B.15. *The adaptive selection of all per-adapter clip thresholds and noise multipliers over the entire training run does not increase the total privacy cost: it remains $(\sum_{t=1}^T \epsilon_t, \sum_{t=1}^T \delta_t)$ -DP.*

Proof. Apply Lemma B.14 at each step t . Since each \mathcal{H}_t uses only the output of $\mathcal{M}_{1:t-1}$, it adds no extra privacy loss. By sequential composition (Theorem B.8), the overall budget remains the sum of the per-step (ϵ_t, δ_t) . \square

4. Enforcement of total budget. In our implementation, we solve via the GDP accountant for a base noise multiplier σ_{base} that ensures

$$\sum_{t=1}^T \epsilon_t = \epsilon_{\text{target}}, \quad \sum_{t=1}^T \delta_t = \delta_{\text{target}}.$$

Because all actual $\sigma_t \geq \sigma_{\text{base}}$ and $C_t^j \leq 1$, each ϵ_t, δ_t can only decrease, so the total remains within budget.

Combining these four points, the full RLDP training algorithm—comprising T DP-SGD steps with adaptive clipping/noise and post-processing updates—satisfies $(\epsilon_{\text{target}}, \delta_{\text{target}})$ -differential privacy. \square